Globális felmelegedés

Fizikai háttér

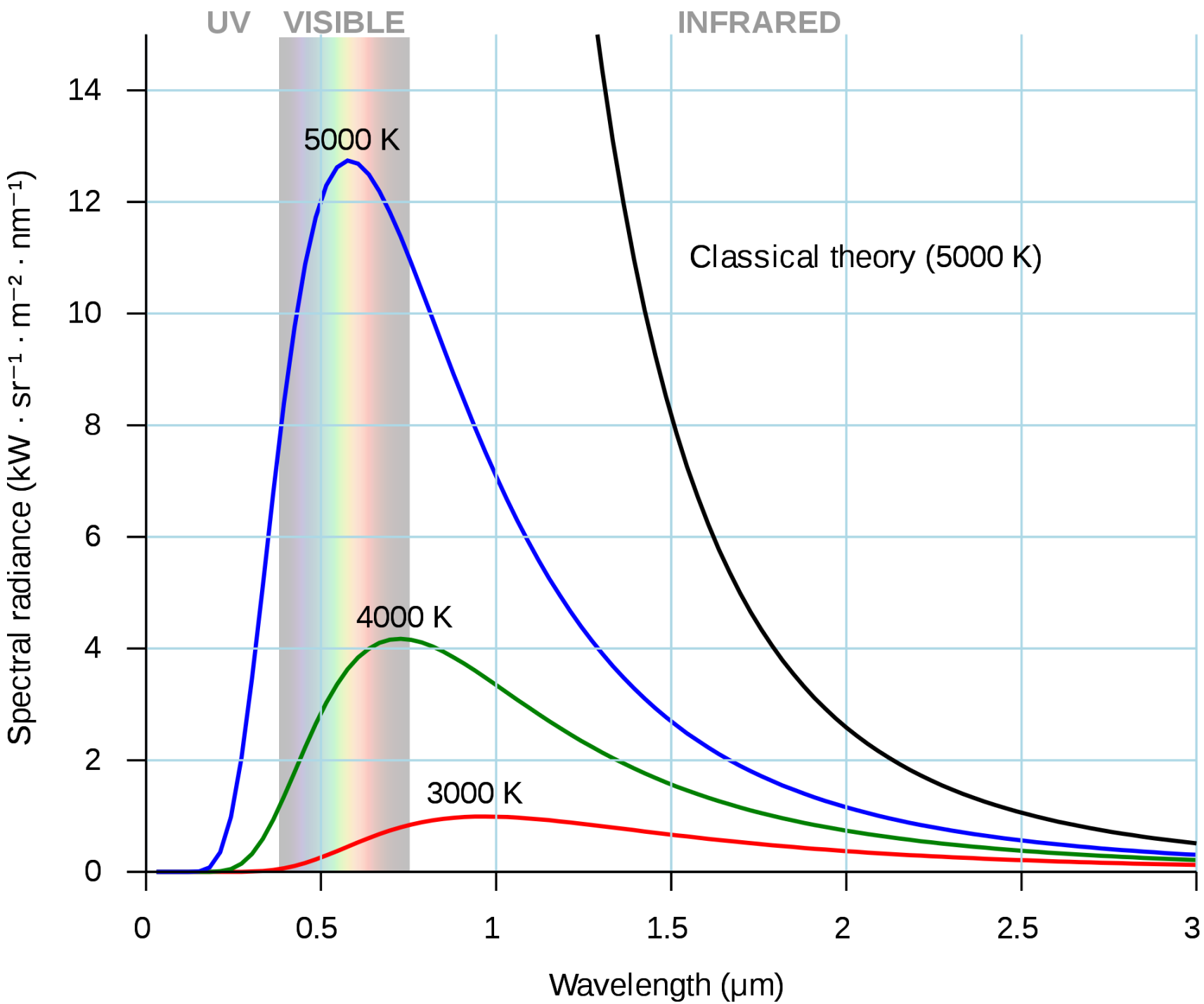

Planck törvény

$$I_\nu(\nu, T) = \frac{2h\nu^3}{c^2} \frac{1}{e^{\frac{h\nu}{kT}} - 1}$$

$$I_\lambda(\lambda, T) = \frac{2hc^2}{\lambda^5} \frac{1}{e^{\frac{hc}{\lambda kT}} - 1}$$

Stefan-Boltzman törvény

$$P = \sigma T^4$$

$$\sigma = 5{,}64 \frac{J}{sm^2K^4}$$

Bolygók hőmérséklete

Háttér, IPCC 2007

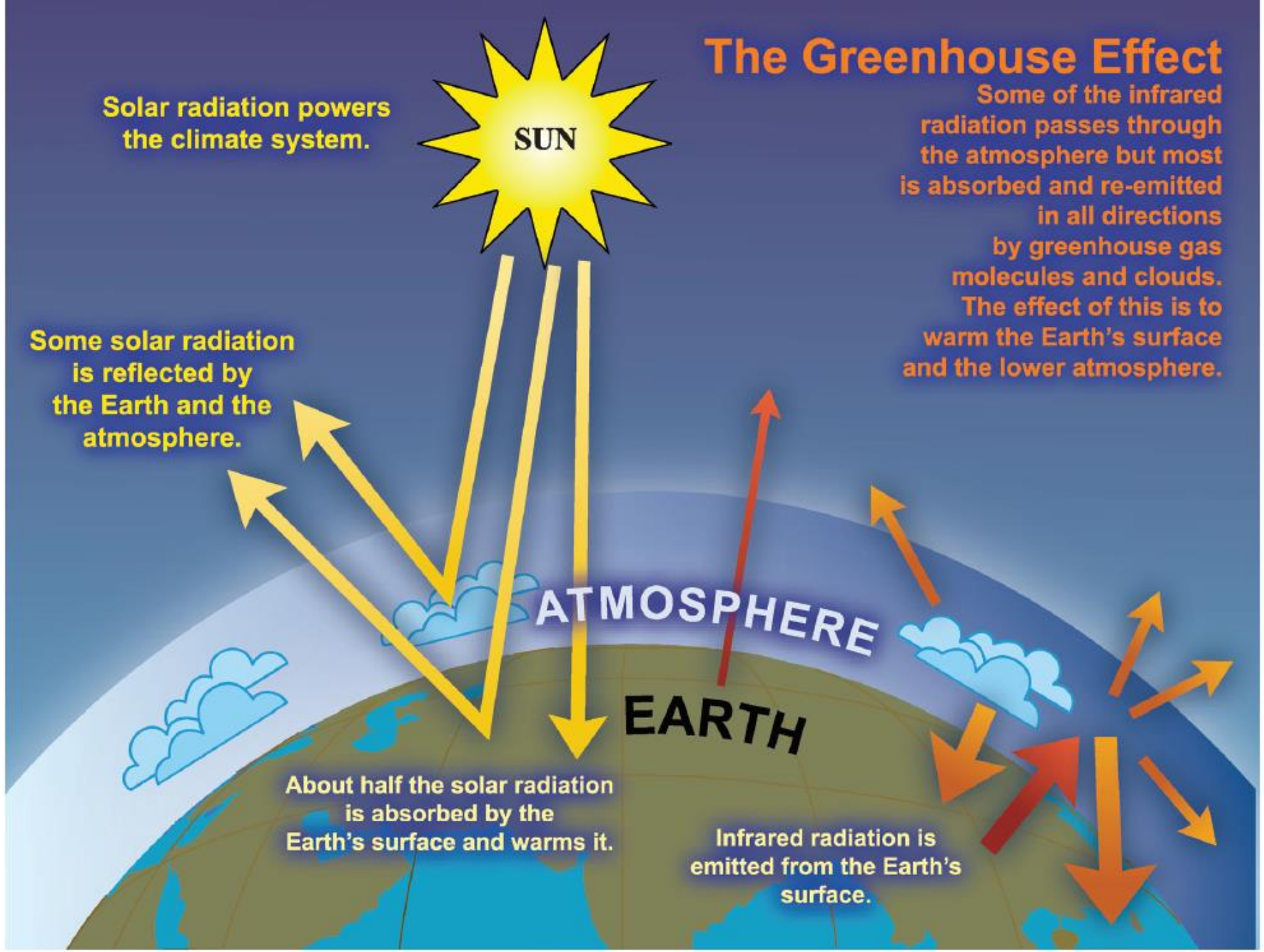

FAQ 1.3, Figure 1. *An idealised model of the natural greenhouse effect. See text for explanation.*

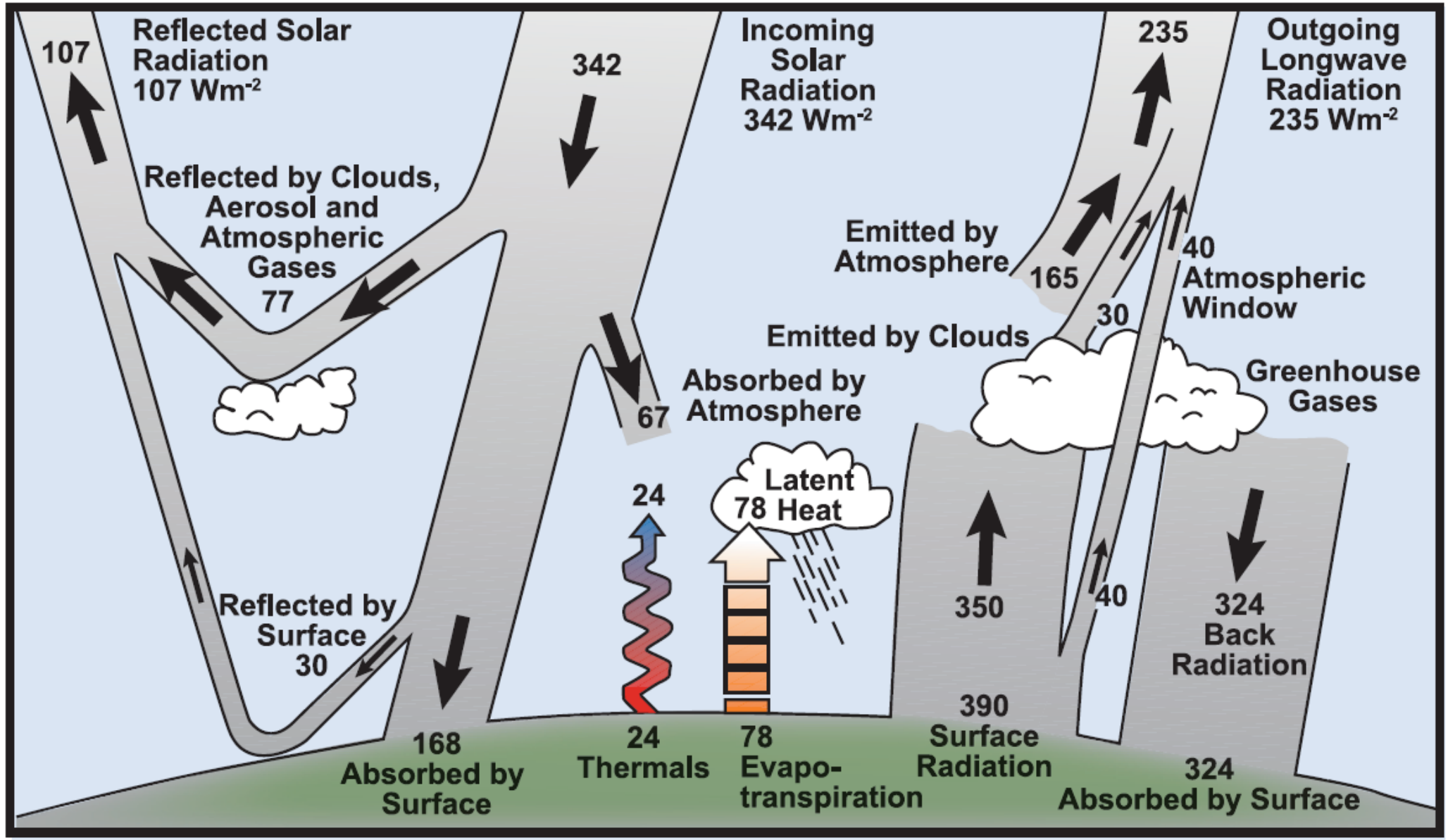

FAQ 1.1, Figure 1. *Estimate of the Earth's annual and global mean energy balance. Over the long term, the amount of incoming solar radiation absorbed by the Earth and atmosphere is balanced by the Earth and atmosphere releasing the same amount of outgoing longwave radiation. About half of the incoming solar radiation is absorbed by the Earth's surface. This energy is transferred to the atmosphere by warming the air in contact with the surface (thermals), by evapotranspiration and by longwave radiation that is absorbed by clouds and greenhouse gases. The atmosphere in turn radiates longwave energy back to Earth as well as out to space. Source: Kiehl and Trenberth (1997).*

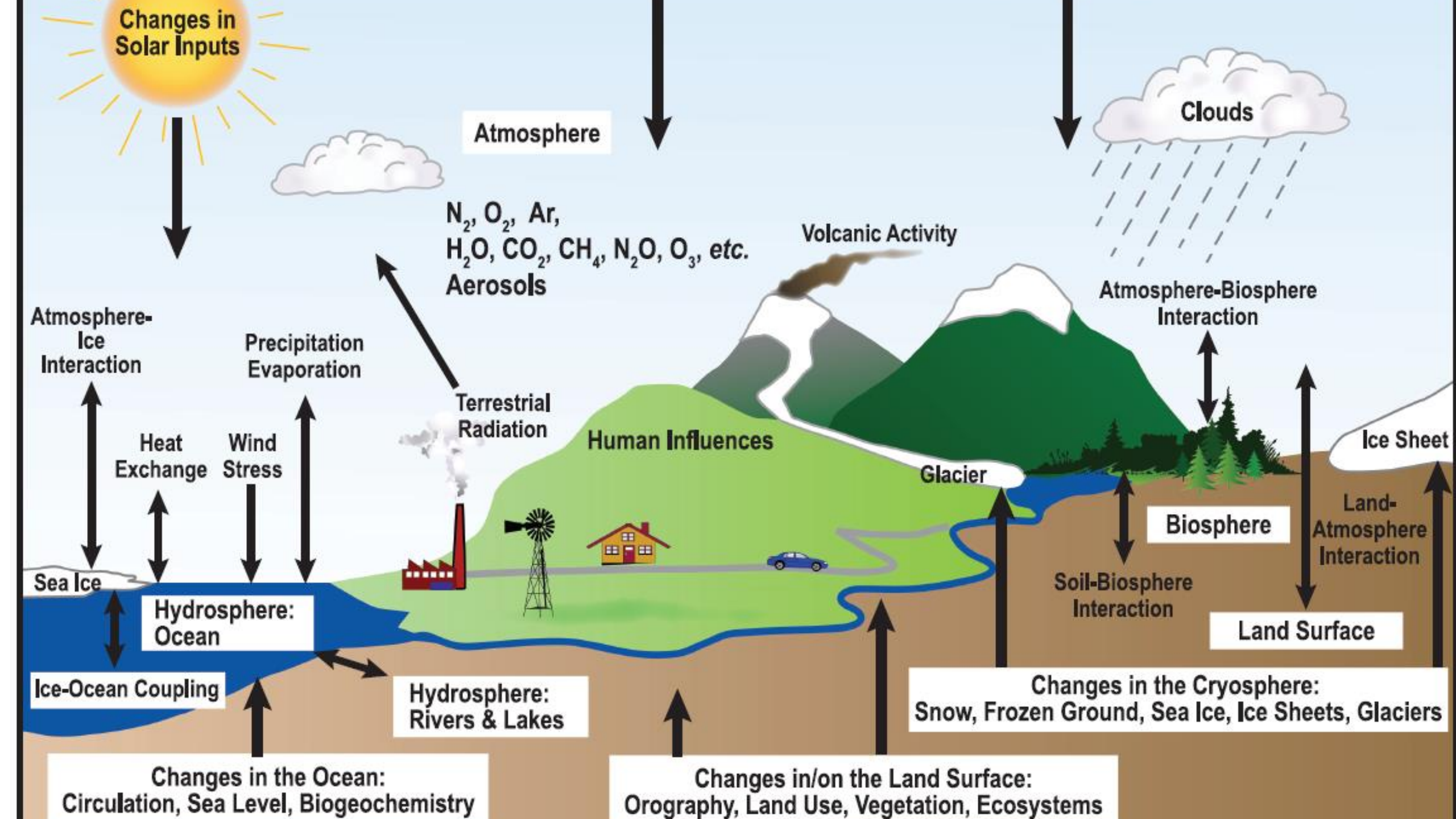
Changes in Solar Inputs
Atmosphere
Clouds
N_2, O_2, Ar,
H_2O, CO_2, CH_4, N_2O, O_3, *etc.*
Aerosols
Volcanic Activity
Atmosphere-Biosphere Interaction
Atmosphere-Ice Interaction
Precipitation Evaporation
Terrestrial Radiation
Heat Exchange
Wind Stress
Human Influences
Glacier
Ice Sheet
Biosphere
Land-Atmosphere Interaction
Sea Ice
Hydrosphere: Ocean
Soil-Biosphere Interaction
Land Surface
Ice-Ocean Coupling
Hydrosphere: Rivers & Lakes
Changes in the Cryosphere: Snow, Frozen Ground, Sea Ice, Ice Sheets, Glaciers
Changes in the Ocean: Circulation, Sea Level, Biogeochemistry
Changes in/on the Land Surface: Orography, Land Use, Vegetation, Ecosystems

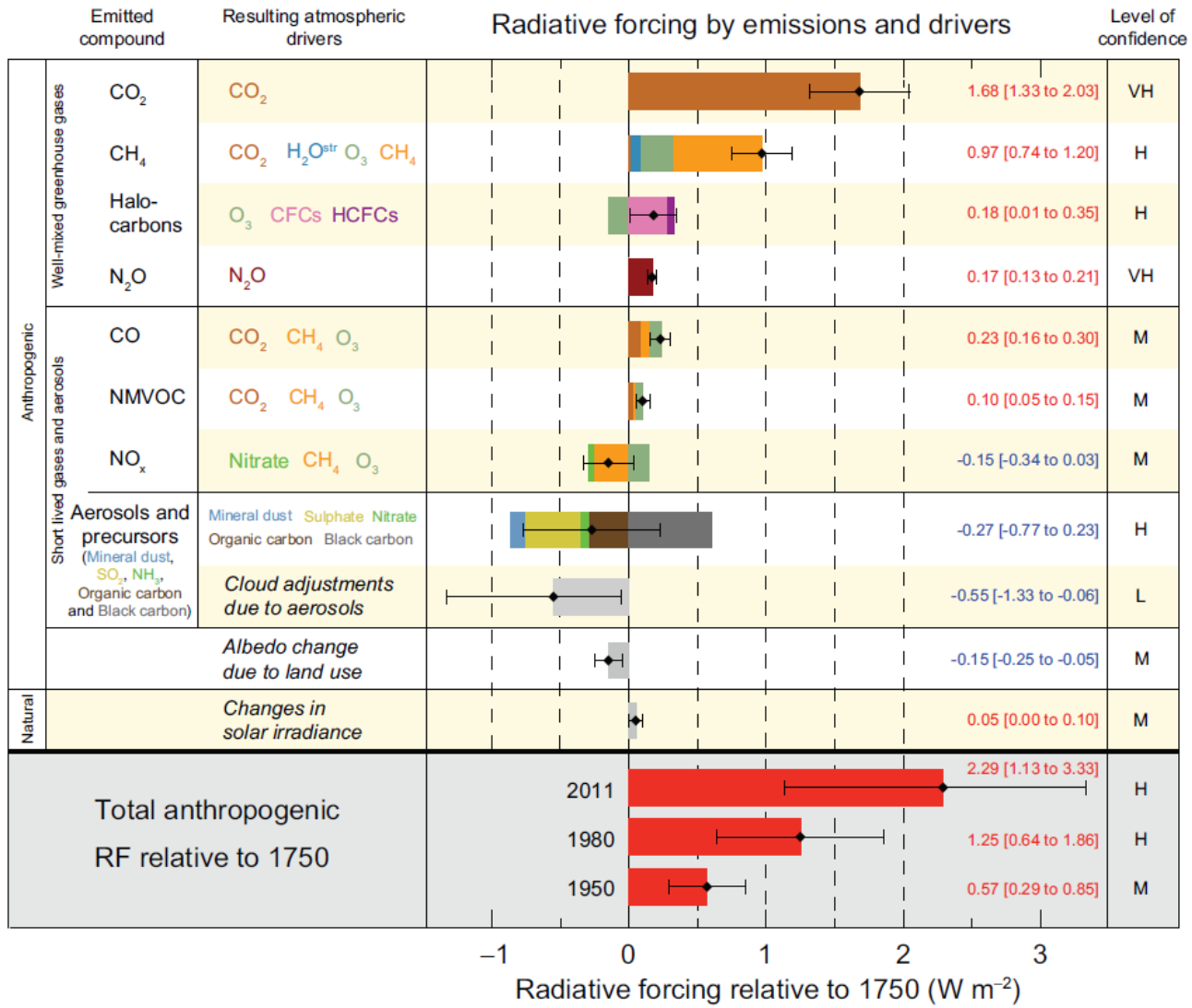

Figure SPM.5 | Radiative forcing estimates in 2011 relative to 1750 and aggregated uncertainties for the main drivers of climate change. Values are global average radiative forcing (RF[14]), partitioned according to the emitted compounds or processes that result in a combination of drivers. The best estimates of the net radiative forcing are shown as black diamonds with corresponding uncertainty intervals; the numerical values are provided on the right of the figure, together with the confidence level in the net forcing (VH – *very high*, H – *high*, M – *medium*, L – *low*, VL – *very low*). Albedo forcing due to black carbon on snow and ice is included in the black carbon aerosol bar. Small forcings due to contrails (0.05 W m^{-2}, including contrail induced cirrus), and HFCs, PFCs and SF_6 (total 0.03 W m^{-2}) are not shown. Concentration-based RFs for gases can be obtained by summing the like-coloured bars. Volcanic forcing is not included as its episodic nature makes is difficult to compare to other forcing mechanisms. Total anthropogenic radiative forcing is provided for three different years relative to 1750. For further technical details, including uncertainty ranges associated with individual components and processes, see the Technical Summary Supplementary Material. {8.5; Figures 8.14–8.18; Figures TS.6 and TS.7}

Részletek, IPCC 2014

Confidence Terminology	Degree of confidence in being correct
Very high confidence	At least 9 out of 10 chance
High confidence	About 8 out of 10 chance
Medium confidence	About 5 out of 10 chance
Low confidence	About 2 out of 10 chance
Very low confidence	Less than 1 out of 10 chance

Likelihood Terminology	Likelihood of the occurrence/ outcome
Virtually certain	> 99% probability
Extremely likely	> 95% probability
Very likely	> 90% probability
Likely	> 66% probability
More likely than not	> 50% probability
About as likely as not	33 to 66% probability
Unlikely	< 33% probability
Very unlikely	< 10% probability
Extremely unlikely	< 5% probability
Exceptionally unlikely	< 1% probability

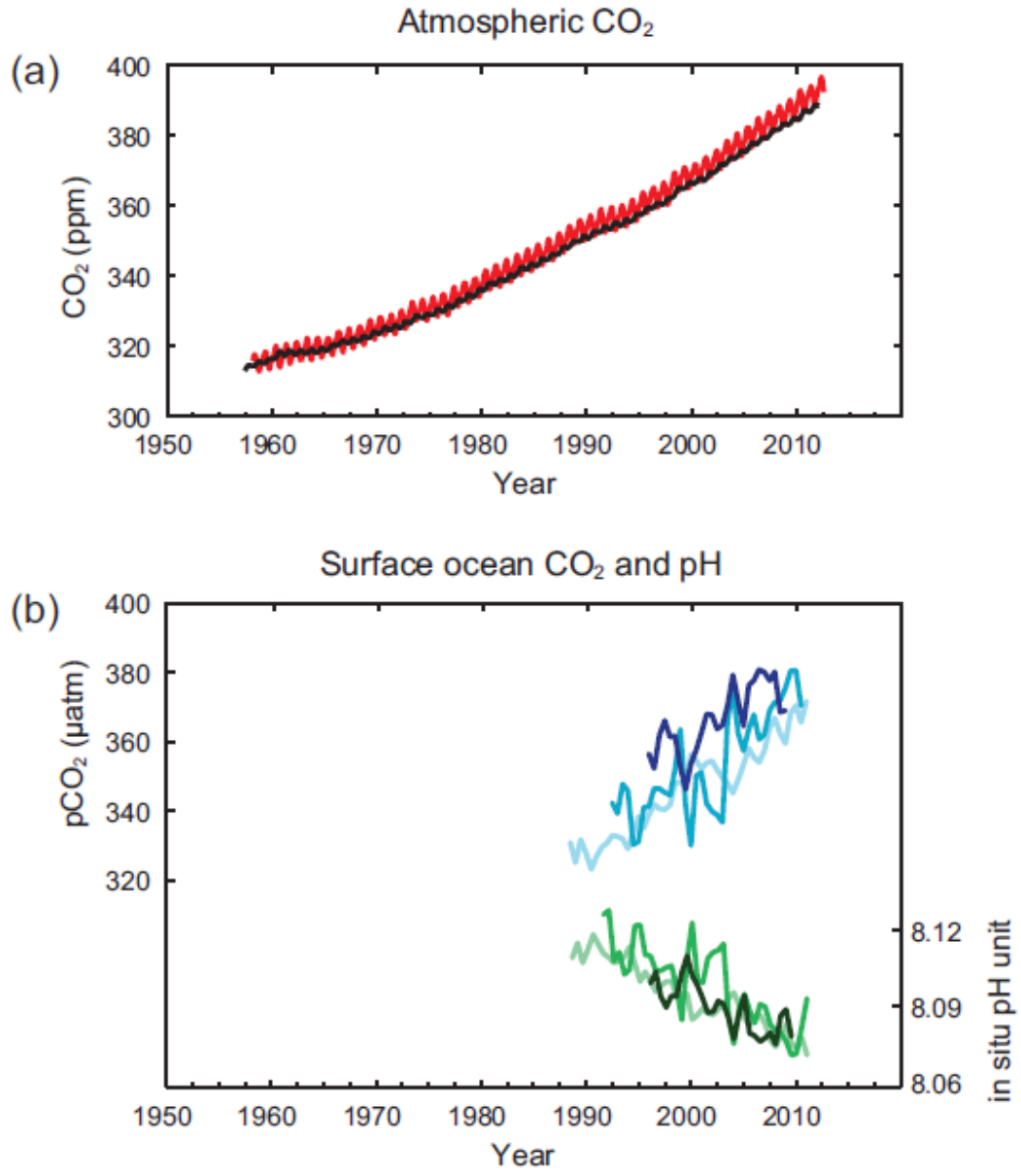

Figure SPM.4 | Multiple observed indicators of a changing global carbon cycle: (a) atmospheric concentrations of carbon dioxide (CO_2) from Mauna Loa (19°32'N, 155°34'W – red) and South Pole (89°59'S, 24°48'W – black) since 1958; (b) partial pressure of dissolved CO_2 at the ocean surface (blue curves) and in situ pH (green curves), a measure of the acidity of ocean water. Measurements are from three stations from the Atlantic (29°10'N, 15°30'W – dark blue/dark green; 31°40'N, 64°10'W – blue/green) and the Pacific Oceans (22°45'N, 158°00'W – light blue/light green). Full details of the datasets shown here are provided in the underlying report and the Technical Summary Supplementary Material. {Figures 2.1 and 3.18; Figure TS.5}

(a)

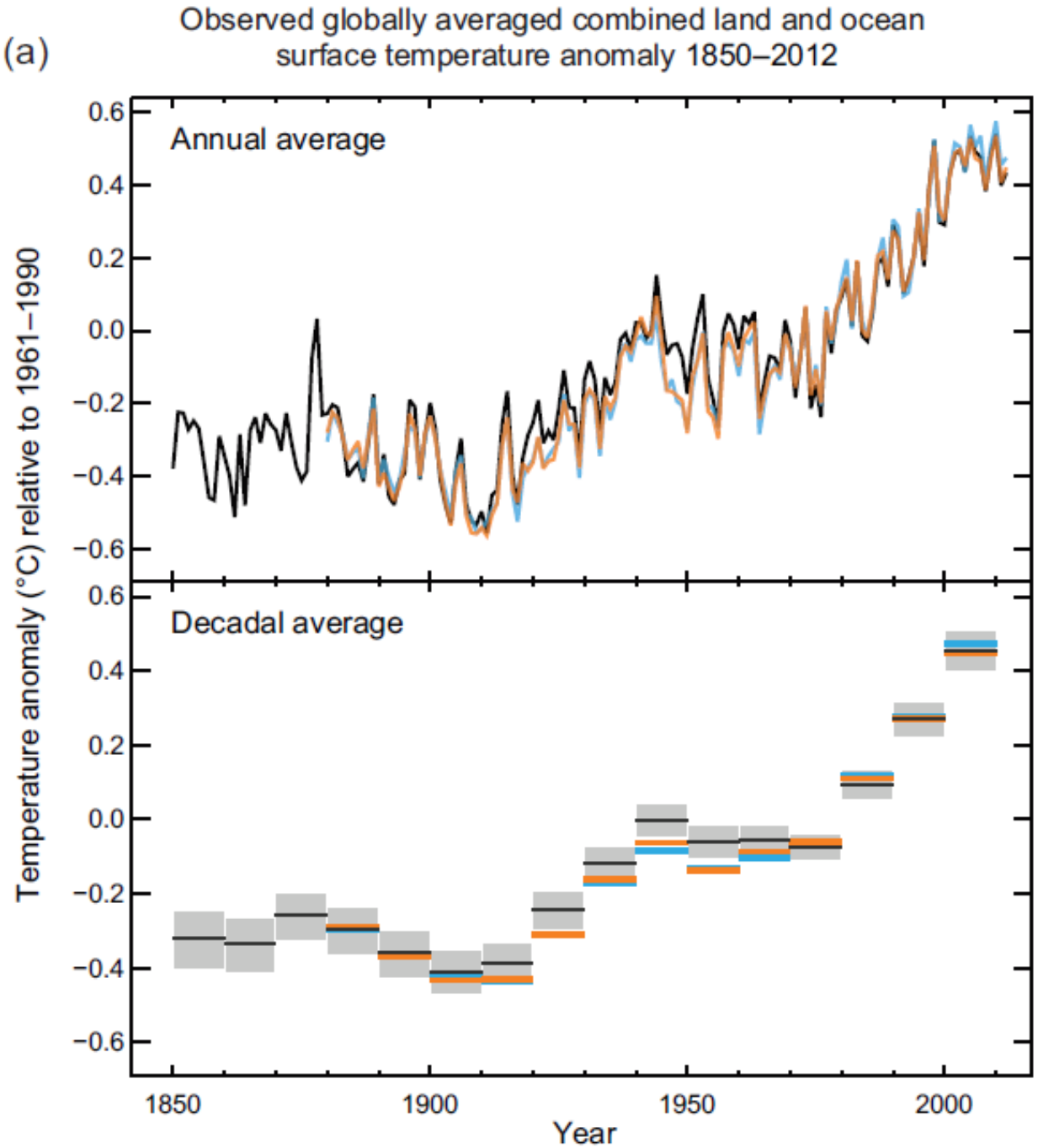
Observed globally averaged combined land and ocean surface temperature anomaly 1850–2012
Annual average
Decadal average
Temperature anomaly (°C) relative to 1961–1990
0.6
0.4
0.2
0.0
−0.2
−0.4
−0.6
1850
1900
1950
2000
Year

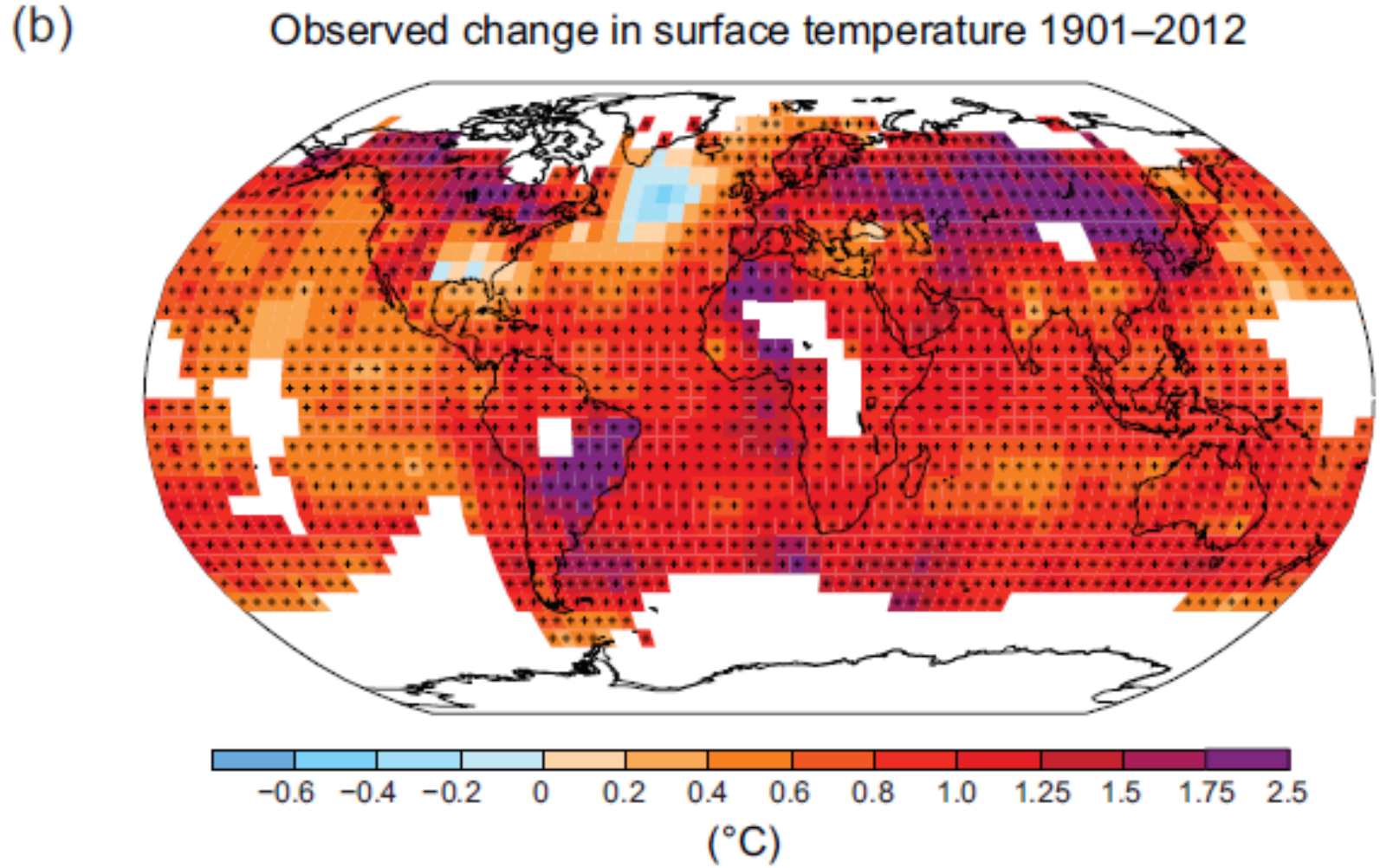

Figure SPM.1 | (a) Observed global mean combined land and ocean surface temperature anomalies, from 1850 to 2012 from three data sets. Top panel: annual mean values. Bottom panel: decadal mean values including the estimate of uncertainty for one dataset (black). Anomalies are relative to the mean of 1961–1990. (b) Map of the observed surface temperature change from 1901 to 2012 derived from temperature trends determined by linear regression from one dataset (orange line in panel a). Trends have been calculated where data availability permits a robust estimate (i.e., only for grid boxes with greater than 70% complete records and more than 20% data availability in the first and last 10% of the time period). Other areas are white. Grid boxes where the trend is significant at the 10% level are indicated by a + sign. For a listing of the datasets and further technical details see the Technical Summary Supplementary Material. {Figures 2.19–2.21; Figure TS.2}

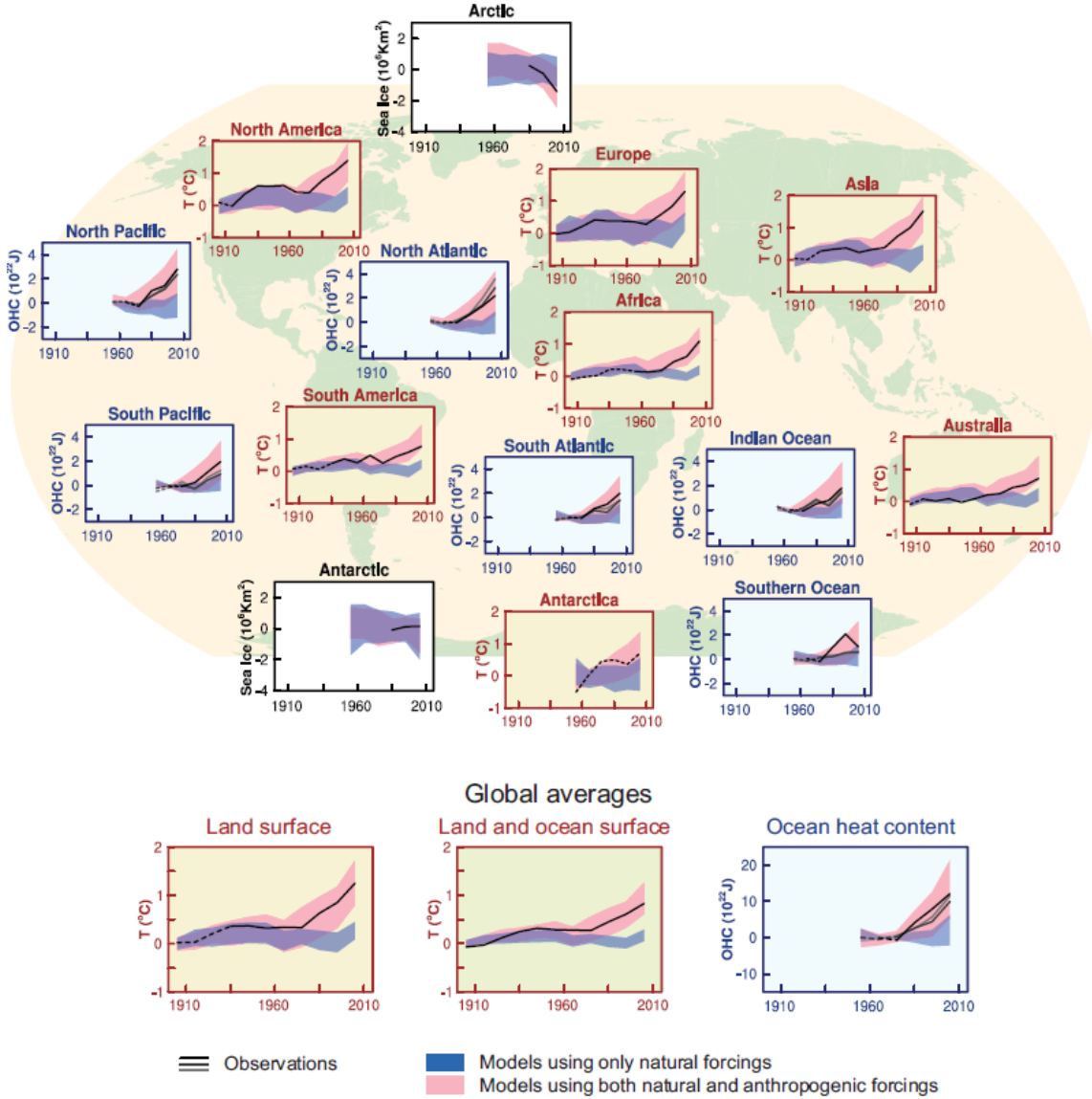

Figure SPM.6 | Comparison of observed and simulated climate change based on three large-scale indicators in the atmosphere, the cryosphere and the ocean: change in continental land surface air temperatures (yellow panels), Arctic and Antarctic September sea ice extent (white panels), and upper ocean heat content in the major ocean basins (blue panels). Global average changes are also given. Anomalies are given relative to 1880–1919 for surface temperatures, 1960–1980 for ocean heat content and 1979–1999 for sea ice. All time-series are decadal averages, plotted at the centre of the decade. For temperature panels, observations are dashed lines if the spatial coverage of areas being examined is below 50%. For ocean heat content and sea ice panels the solid line is where the coverage of data is good and higher in quality, and the dashed line is where the data coverage is only adequate, and thus, uncertainty is larger. Model results shown are Coupled Model Intercomparison Project Phase 5 (CMIP5) multi-model ensemble ranges, with shaded bands indicating the 5 to 95% confidence intervals. For further technical details, including region definitions see the Technical Summary Supplementary Material. {Figure 10.21; Figure TS.12}

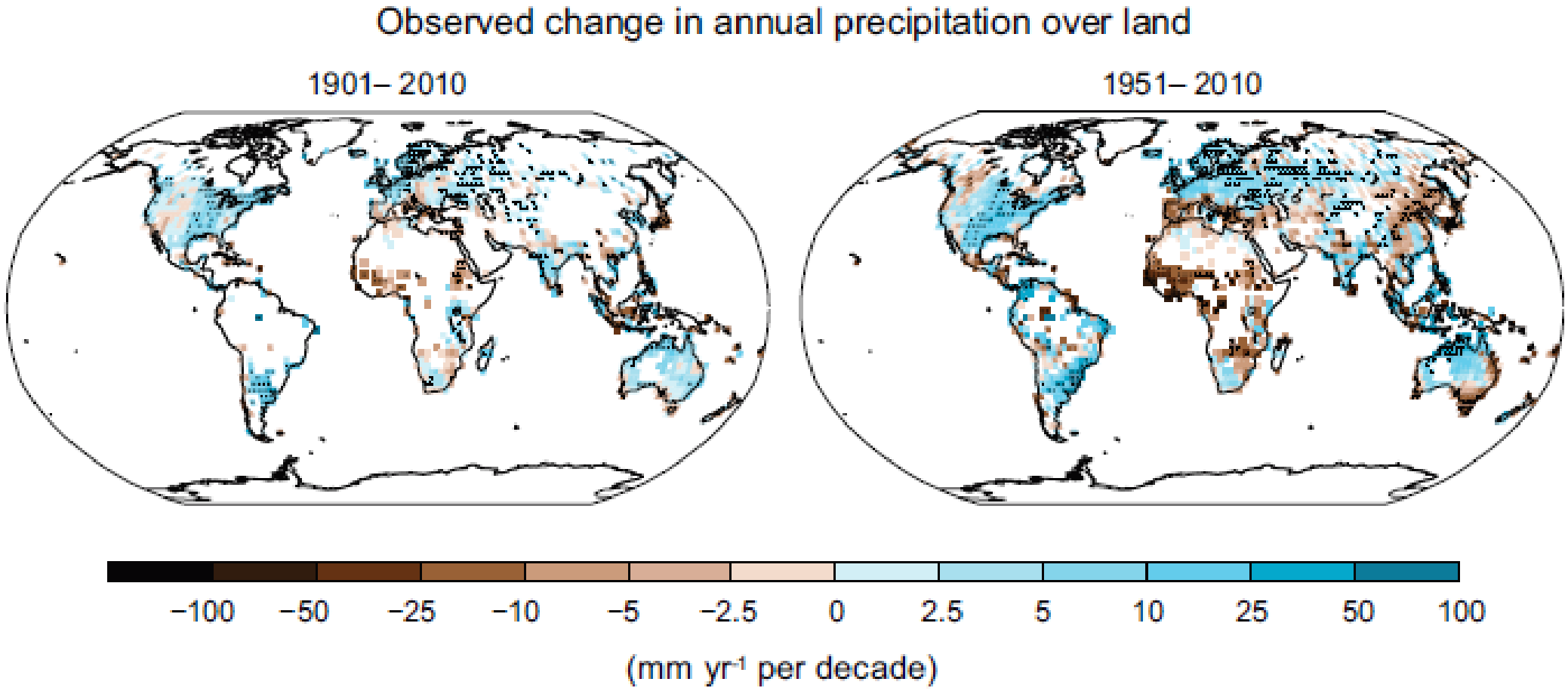

Figure SPM.2 | Maps of observed precipitation change from 1901 to 2010 and from 1951 to 2010 (trends in annual accumulation calculated using the same criteria as in Figure SPM.1) from one data set. For further technical details see the Technical Summary Supplementary Material. {TS TFE.1, Figure 2; Figure 2.29}

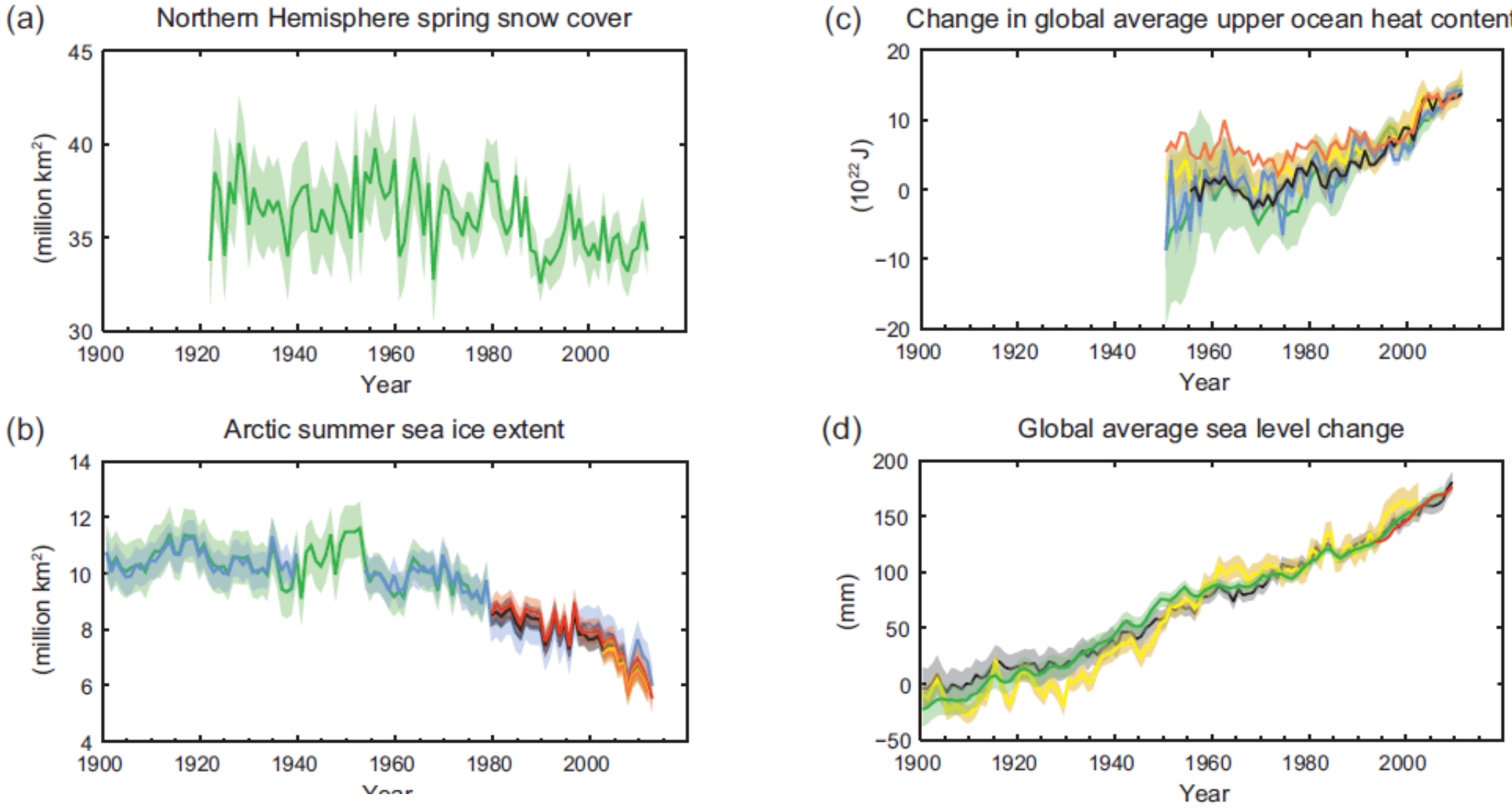

Figure SPM.3 | Multiple observed indicators of a changing global climate: (a) Extent of Northern Hemisphere March-April (spring) average snow cover; (b) extent of Arctic July-August-September (summer) average sea ice; (c) change in global mean upper ocean (0–700 m) heat content aligned to 2006–2010, and relative to the mean of all datasets for 1970; (d) global mean sea level relative to the 1900–1905 mean of the longest running dataset, and with all datasets aligned to have the same value in 1993, the first year of satellite altimetry data. All time-series (coloured lines indicating different data sets) show annual values, and where assessed, uncertainties are indicated by coloured shading. See Technical Summary Supplementary Material for a listing of the datasets. {Figures 3.2, 3.13, 4.19, and 4.3; FAQ 2.1, Figure 2; Figure TS.1}

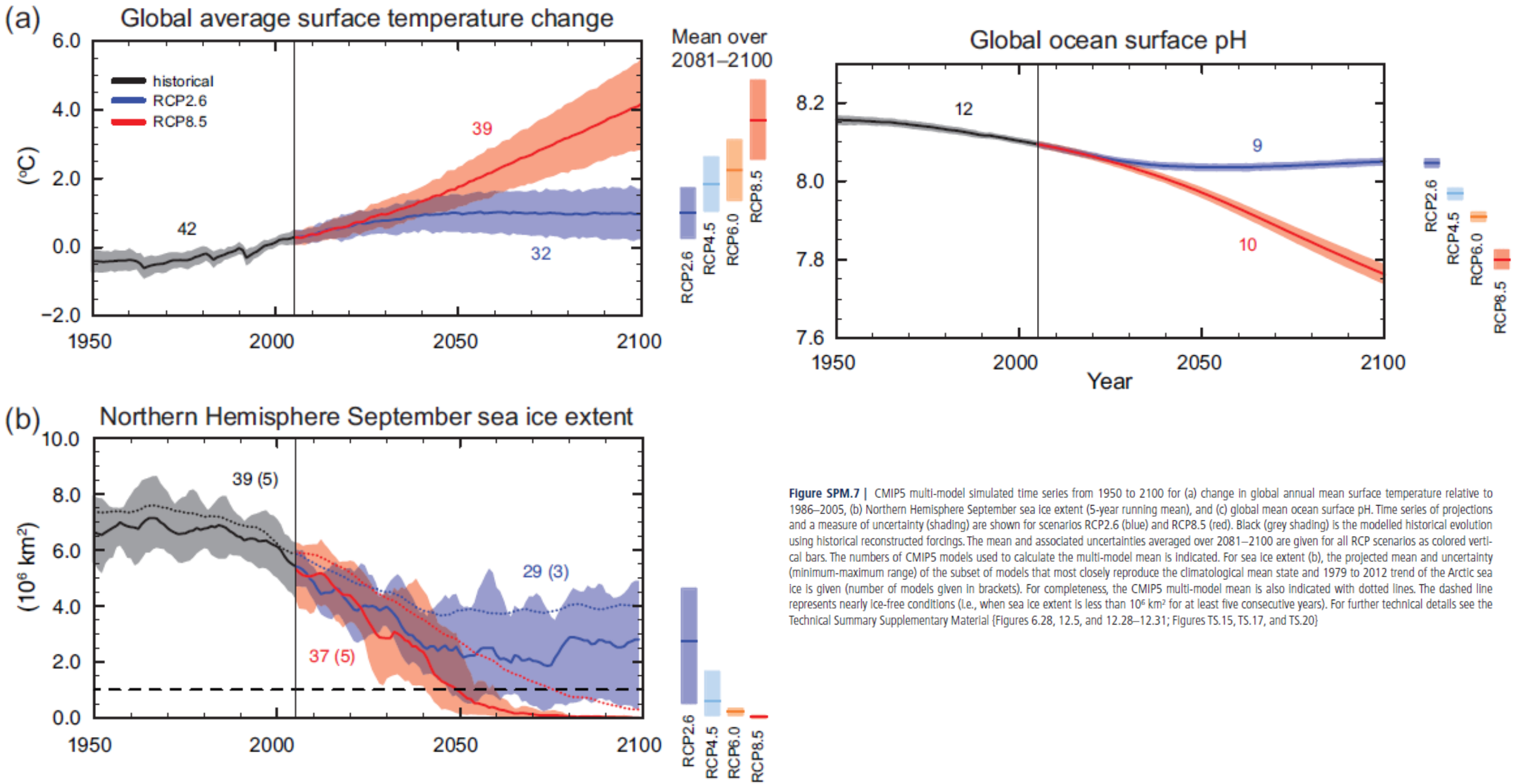

Figure SPM.7 | CMIP5 multi-model simulated time series from 1950 to 2100 for (a) change in global annual mean surface temperature relative to 1986–2005, (b) Northern Hemisphere September sea ice extent (5-year running mean), and (c) global mean ocean surface pH. Time series of projections and a measure of uncertainty (shading) are shown for scenarios RCP2.6 (blue) and RCP8.5 (red). Black (grey shading) is the modelled historical evolution using historical reconstructed forcings. The mean and associated uncertainties averaged over 2081–2100 are given for all RCP scenarios as colored vertical bars. The numbers of CMIP5 models used to calculate the multi-model mean is indicated. For sea ice extent (b), the projected mean and uncertainty (minimum-maximum range) of the subset of models that most closely reproduce the climatological mean state and 1979 to 2012 trend of the Arctic sea ice is given (number of models given in brackets). For completeness, the CMIP5 multi-model mean is also indicated with dotted lines. The dashed line represents nearly ice-free conditions (i.e., when sea ice extent is less than 10^6 km^2 for at least five consecutive years). For further technical details see the Technical Summary Supplementary Material {Figures 6.28, 12.5, and 12.28–12.31; Figures TS.15, TS.17, and TS.20}

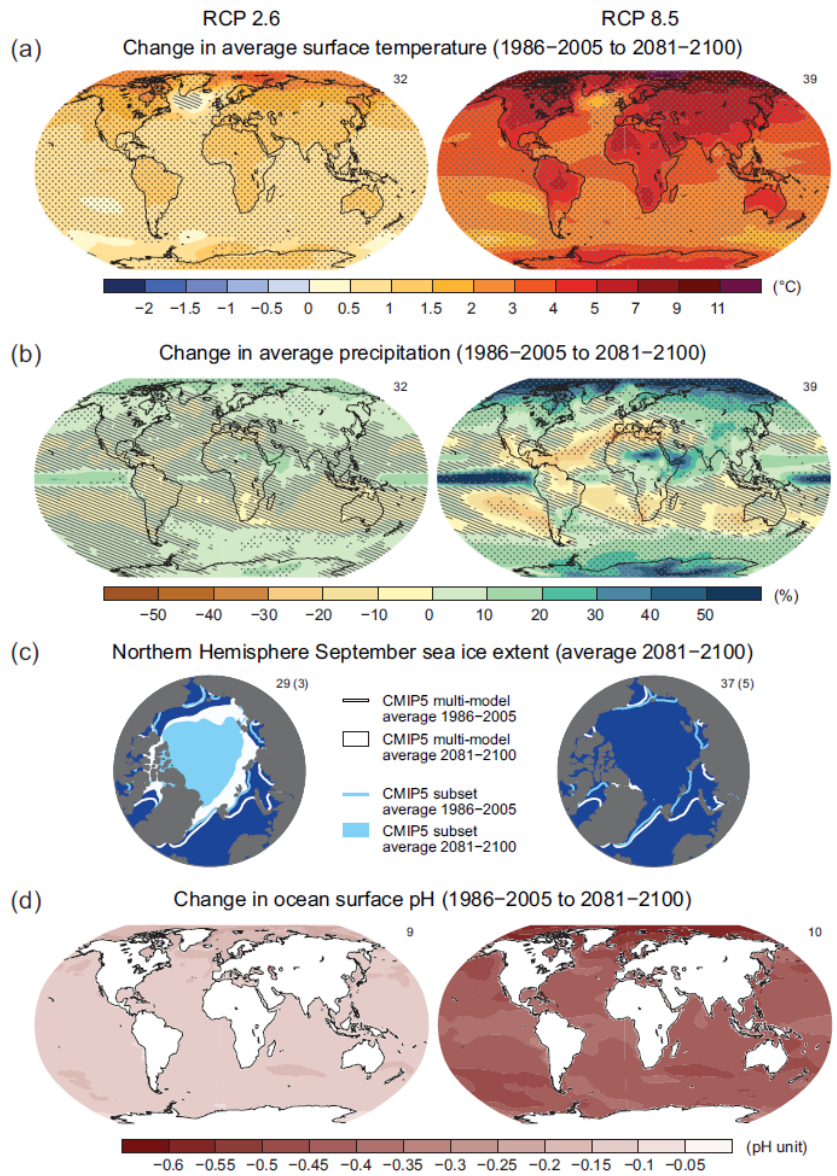

Figure SPM.8 | Maps of CMIP5 multi-model mean results for the scenarios RCP2.6 and RCP8.5 in 2081–2100 of (a) annual mean surface temperature change, (b) average percent change in annual mean precipitation, (c) Northern Hemisphere September sea ice extent, and (d) change in ocean surface pH. Changes in panels (a), (b) and (d) are shown relative to 1986–2005. The number of CMIP5 models used to calculate the multi-model mean is indicated in the upper right corner of each panel. For panels (a) and (b), hatching indicates regions where the multi-model mean is small compared to natural internal variability (i.e., less than one standard deviation of natural internal variability in 20-year means). Stippling indicates regions where the multi-model mean is large compared to natural internal variability (i.e., greater than two standard deviations of natural internal variability in 20-year means) and where at least 90% of models agree on the sign of change (see Box 12.1). In panel (c), the lines are the modelled means for 1986–2005; the filled areas are for the end of the century. The CMIP5 multi-model mean is given in white colour, the projected mean sea ice extent of a subset of models (number of models given in brackets) that most closely reproduce the climatological mean state and 1979 to 2012 trend of the Arctic sea ice extent is given in light blue colour. For further technical details see the Technical Summary Supplementary Material. {Figures 6.28, 12.11, 12.22, and 12.29; Figures TS.15, TS.16, TS.17, and TS.20}

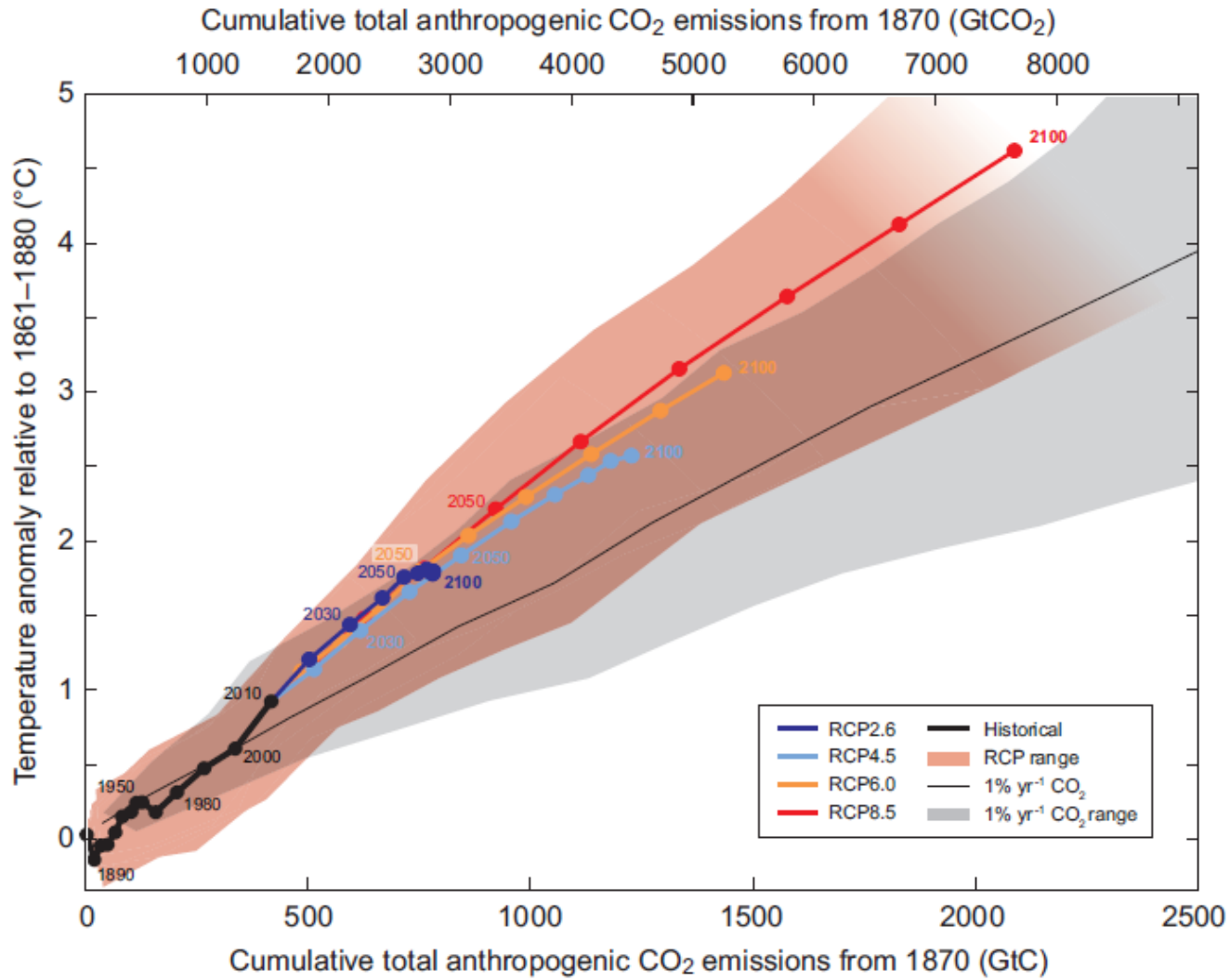

Figure SPM.10 | Global mean surface temperature increase as a function of cumulative total global CO_2 emissions from various lines of evidence. Multi-model results from a hierarchy of climate-carbon cycle models for each RCP until 2100 are shown with coloured lines and decadal means (dots). Some decadal means are labeled for clarity (e.g., 2050 indicating the decade 2040–2049). Model results over the historical period (1860 to 2010) are indicated in black. The coloured plume illustrates the multi-model spread over the four RCP scenarios and fades with the decreasing number of available models in RCP8.5. The multi-model mean and range simulated by CMIP5 models, forced by a CO_2 increase of 1% per year (1% yr^{-1} CO_2 simulations), is given by the thin black line and grey area. For a specific amount of cumulative CO_2 emissions, the 1% per year CO_2 simulations exhibit lower warming than those driven by RCPs, which include additional non-CO_2 forcings. Temperature values are given relative to the 1861–1880 base period, emissions relative to 1870. Decadal averages are connected by straight lines. For further technical details see the Technical Summary Supplementary Material. {Figure 12.45; TS TFE.8, Figure 1}

Hatások, IPCC 2014

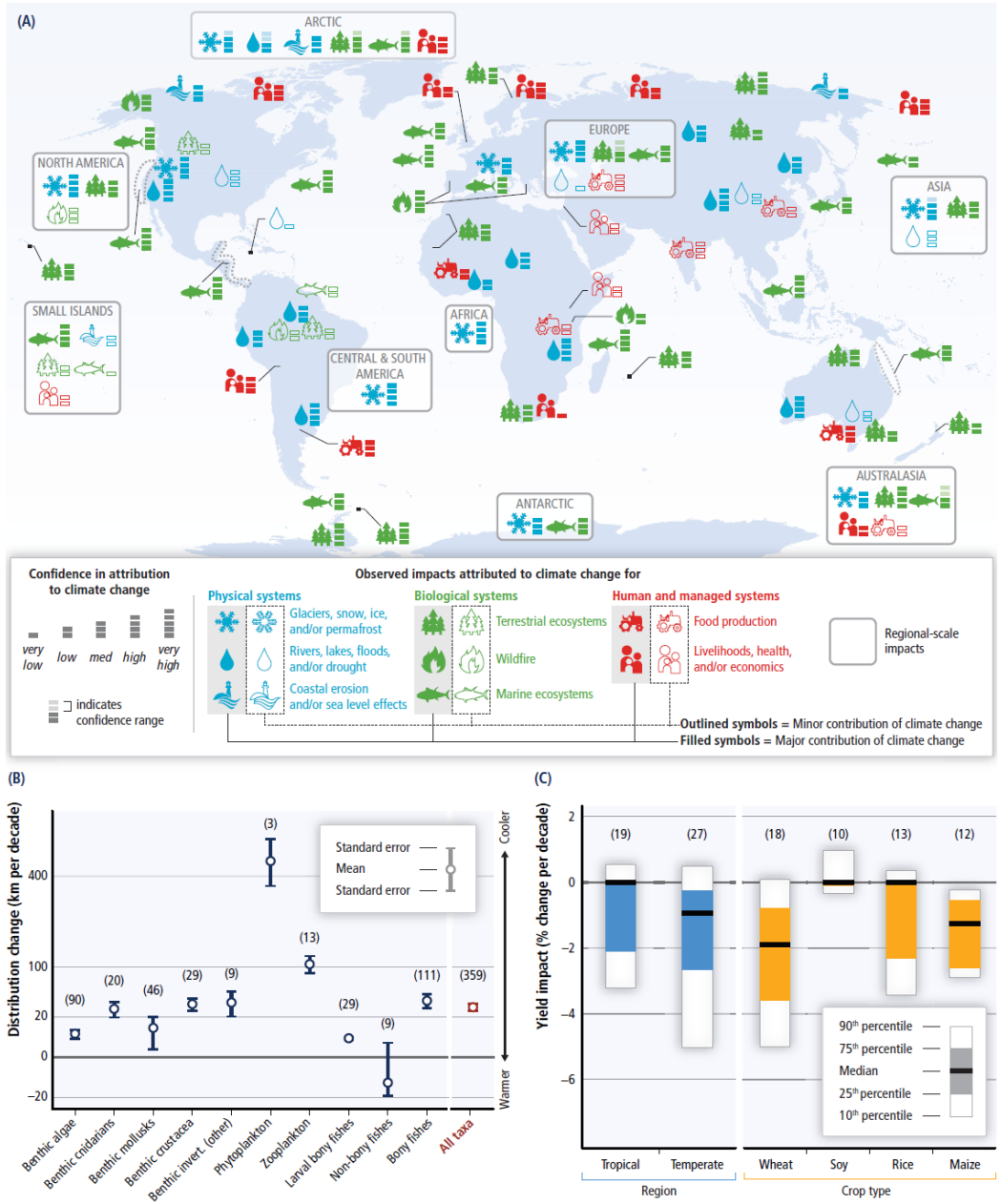

Figure SPM.2 | Widespread impacts in a changing world. (A) Global patterns of impacts in recent decades attributed to climate change, based on studies since the AR4. Impacts are shown at a range of geographic scales. Symbols indicate categories of attributed impacts, the relative contribution of climate change (major or minor) to the observed impact, and confidence in attribution. See supplementary Table SPM.A1 for descriptions of the impacts. (B) Average rates of change in distribution (km per decade) for marine taxonomic groups based on observations over 1900–2010. Positive distribution changes are consistent with warming (moving into previously cooler waters, generally poleward). The number of responses analyzed is given within parentheses for each category. (C) Summary of estimated impacts of observed climate changes on yields over 1960–2013 for four major crops in temperate and tropical regions, with the number of data points analyzed given within parentheses for each category. [Figures 7-2, 18-3, and MB-2]

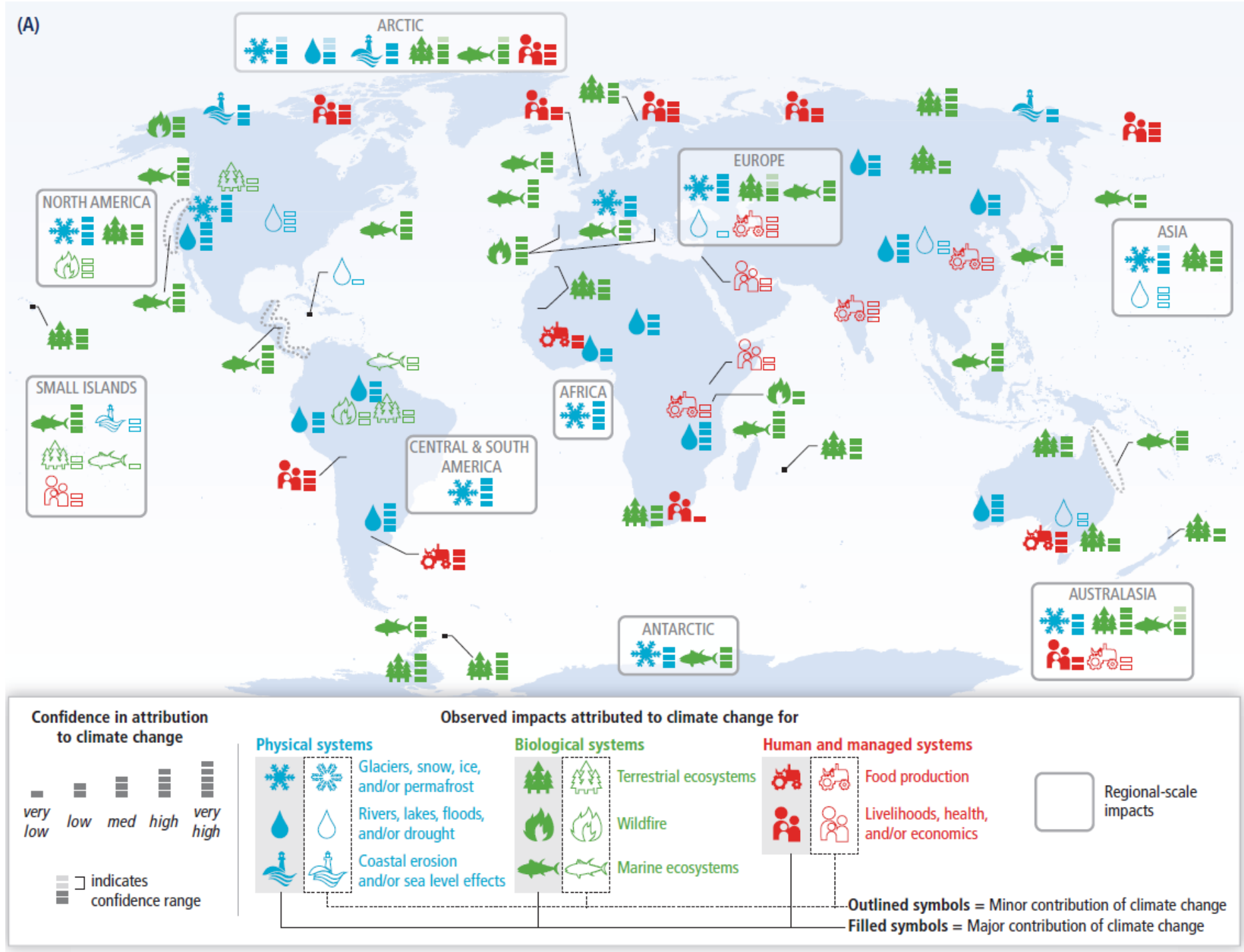
(A)
ARCTIC
NORTH AMERICA
EUROPE
ASIA
SMALL ISLANDS
AFRICA
CENTRAL & SOUTH AMERICA
ANTARCTIC
AUSTRALASIA
Confidence in attribution to climate change
very low
low
med
high
very high
indicates confidence range
Observed impacts attributed to climate change for
Physical systems
Glaciers, snow, ice, and/or permafrost
Rivers, lakes, floods, and/or drought
Coastal erosion and/or sea level effects
Biological systems
Terrestrial ecosystems
Wildfire
Marine ecosystems
Human and managed systems
Food production
Livelihoods, health, and/or economics
Regional-scale impacts
Outlined symbols = Minor contribution of climate change
Filled symbols = Major contribution of climate change

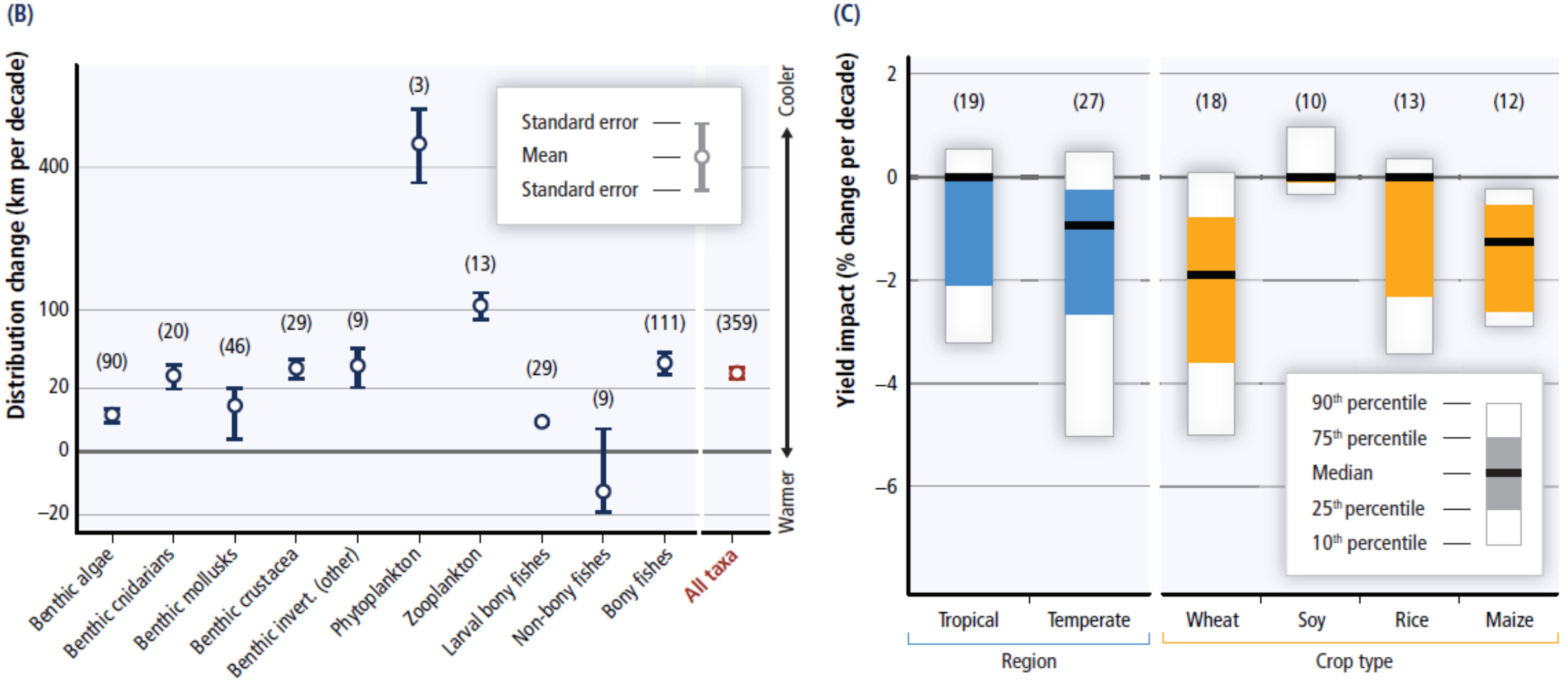

Figure SPM.2 | Widespread impacts in a changing world. (A) Global patterns of impacts in recent decades attributed to climate change, based on studies since the AR4. Impacts are shown at a range of geographic scales. Symbols indicate categories of attributed impacts, the relative contribution of climate change (major or minor) to the observed impact, and confidence in attribution. See supplementary Table SPM.A1 for descriptions of the impacts. (B) Average rates of change in distribution (km per decade) for marine taxonomic groups based on observations over 1900–2010. Positive distribution changes are consistent with warming (moving into previously cooler waters, generally poleward). The number of responses analyzed is given within parentheses for each category. (C) Summary of estimated impacts of observed climate changes on yields over 1960–2013 for four major crops in temperate and tropical regions, with the number of data points analyzed given within parentheses for each category. [Figures 7-2, 18-3, and MB-2]

Observed Temperature Change

Based on trend over 1901–2012 (°C over period)

Solid Color	Significant trend
White	Insufficient data
Diagonal Lines	Trend not statistically significant

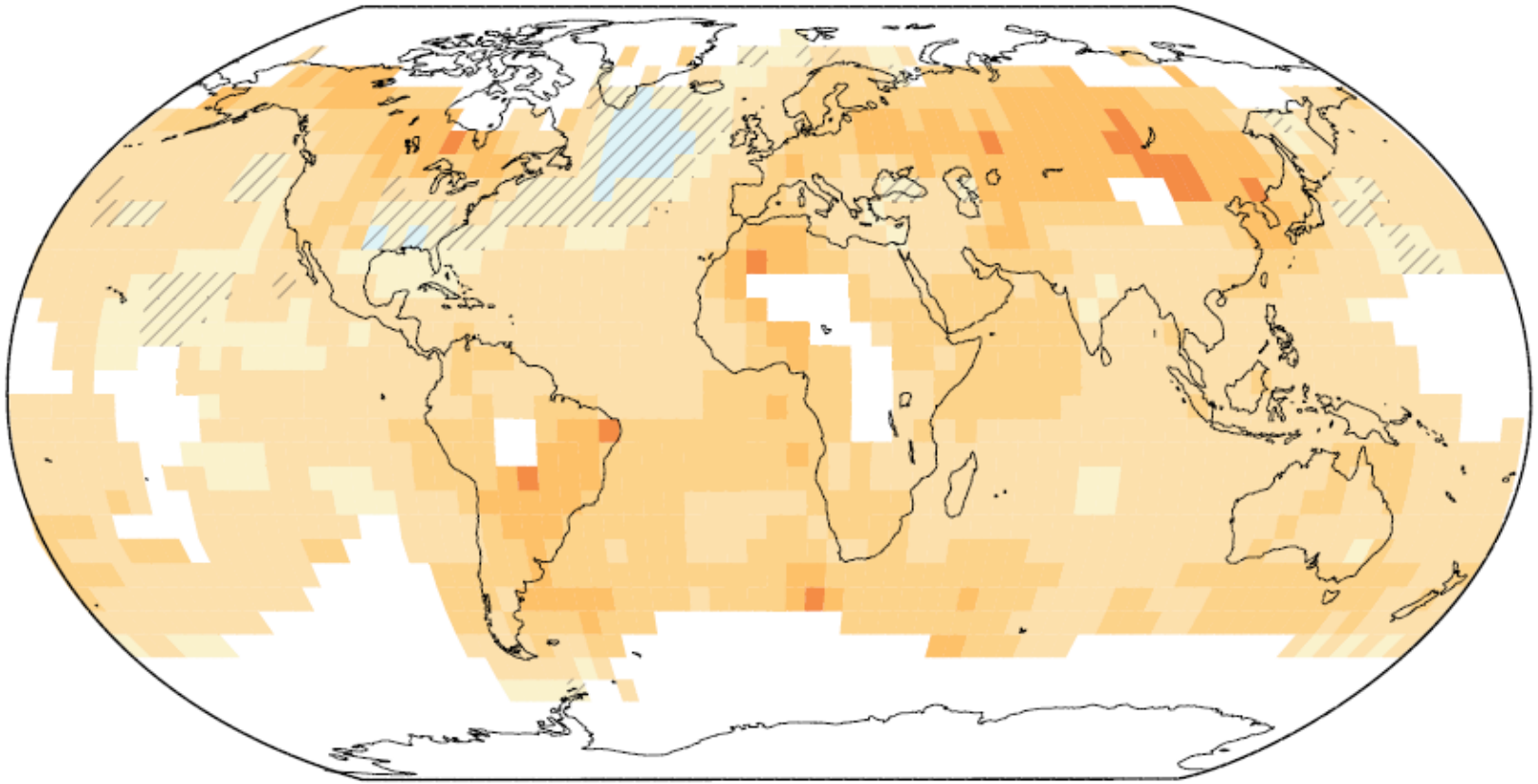

(B)

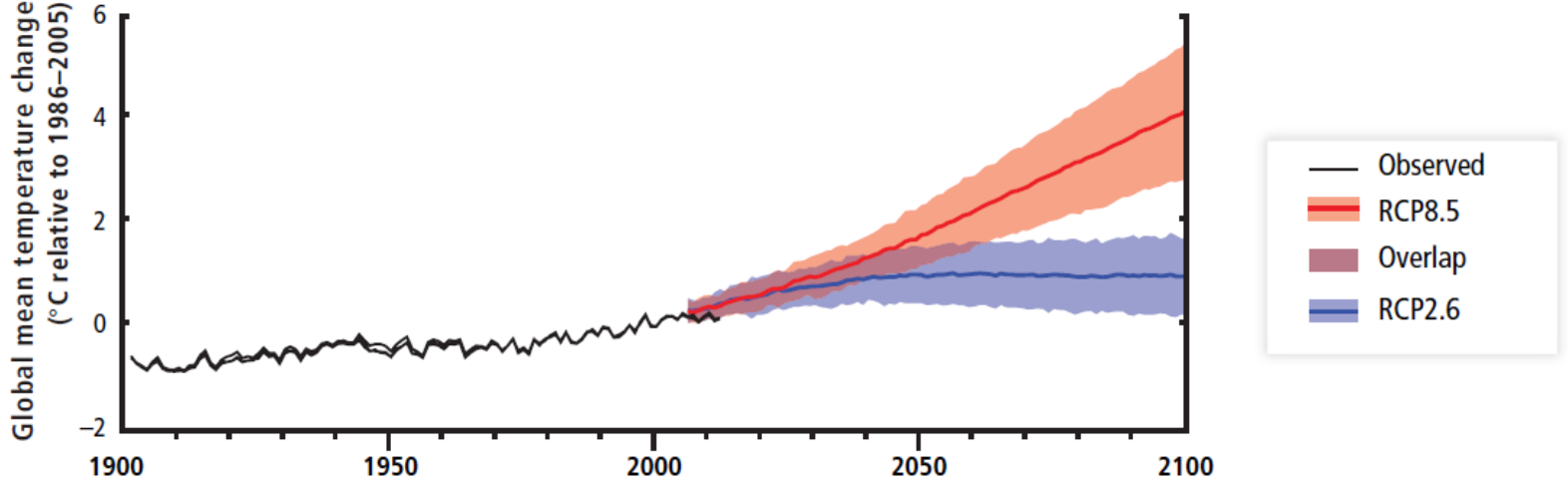

(C)

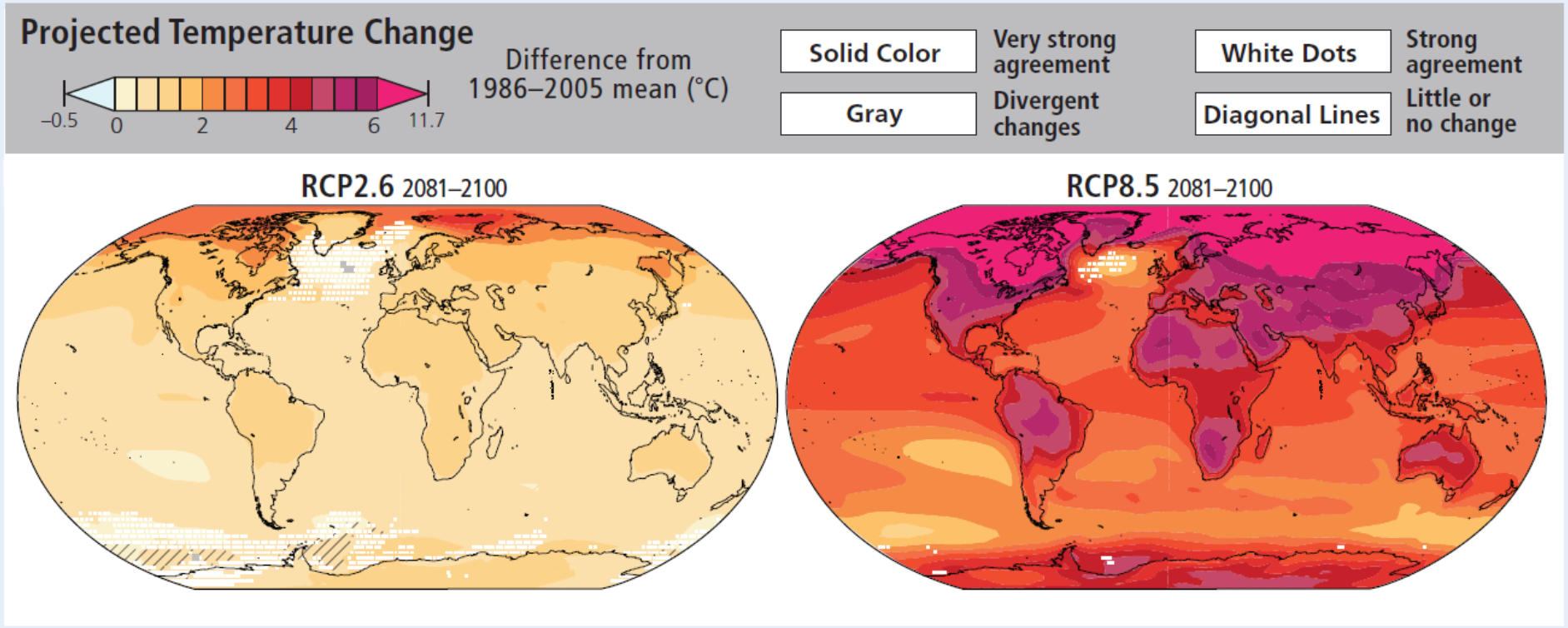

Figure SPM.4 | Observed and projected changes in annual average surface temperature. This figure informs understanding of climate-related risks in the WGII AR5. It illustrates temperature change observed to date and projected warming under continued high emissions and under ambitious mitigation.

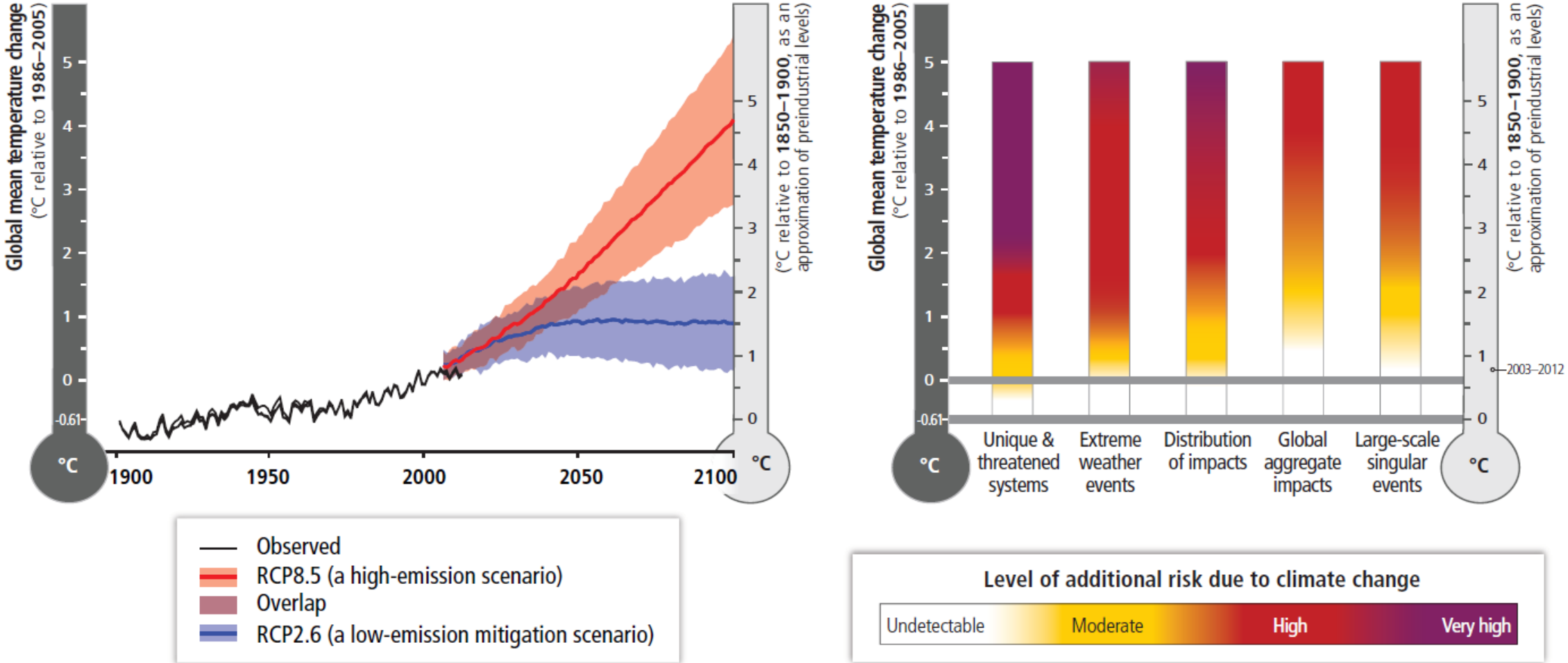

Assessment Box SPM.1 Figure 1 | A global perspective on climate-related risks. Risks associated with reasons for concern are shown at right for increasing levels of climate change. The color shading indicates the additional risk due to climate change when a temperature level is reached and then sustained or exceeded. Undetectable risk (white) indicates no associated impacts are detectable and attributable to climate change. Moderate risk (yellow) indicates that associated impacts are both detectable and attributable to climate change with at least *medium confidence*, also accounting for the other specific criteria for key risks. High risk (red) indicates severe and widespread impacts, also accounting for the other specific criteria for key risks. Purple, introduced in this assessment, shows that very high risk is indicated by all specific criteria for key risks. [Figure 19-4] For reference, past and projected global annual average surface temperature is shown at left, as in Figure SPM.4. [Figure RC-1, Box CC-RC; WGI AR5 Figures SPM.1 and SPM.7] Based on the longest global surface temperature dataset available, the observed change between the average of the period 1850–1900 and of the AR5 reference period (1986–2005) is 0.61°C (5–95% confidence interval: 0.55 to 0.67°C) [WGI AR5 SPM, 2.4], which is used here as an approximation of the change in global mean surface temperature since preindustrial times, referred to as the period before 1750. [WGI and WGII AR5 glossaries]

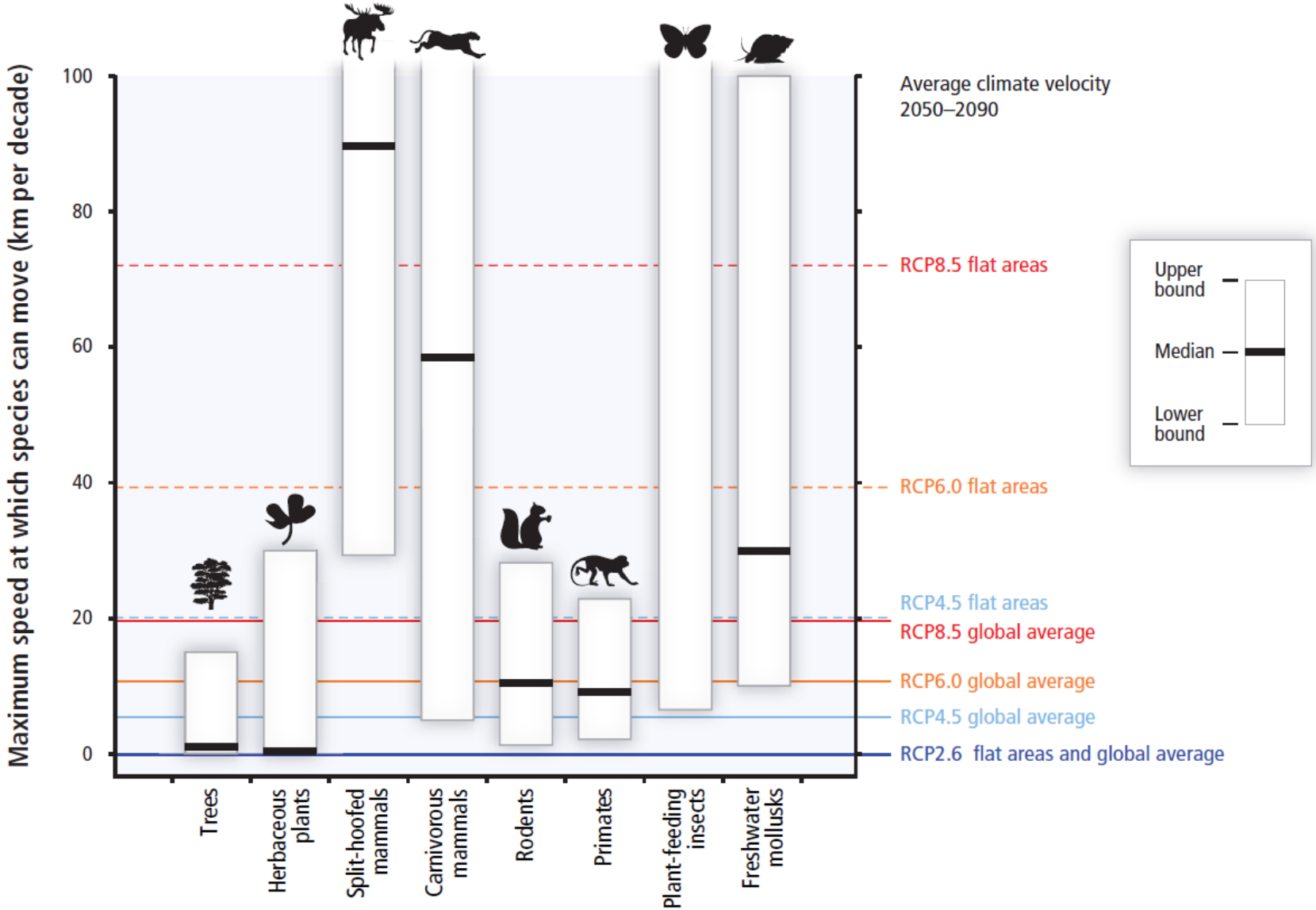

Figure SPM.5 | Maximum speeds at which species can move across landscapes (based on observations and models; vertical axis on left), compared with speeds at which temperatures are projected to move across landscapes (climate velocities for temperature; vertical axis on right). Human interventions, such as transport or habitat fragmentation can greatly increase or decrease speeds of movement. White boxes with black bars indicate ranges and medians of maximum movement speeds for trees, plants, mammals, plant-feeding insects (median not estimated), and freshwater mollusks. For RCP2.6, 4.5, 6.0, and 8.5 for 2050–2090, horizontal lines show climate velocity for the global-land-area average and for large flat regions. Species with maximum speeds below each line are expected to be unable to track warming in the absence of human intervention. [Figure 4-5]

Mi a teendő? ICCP 2014

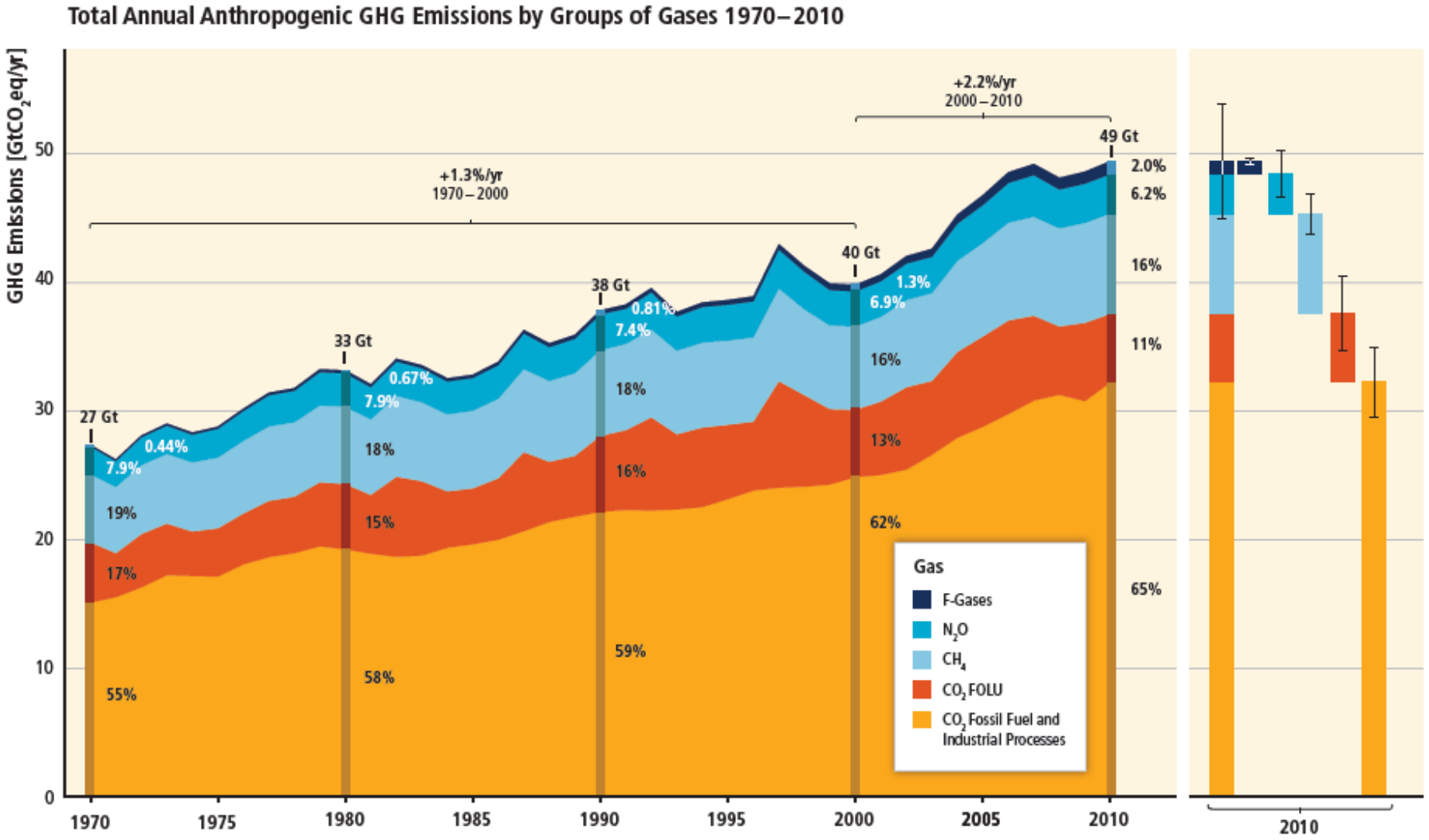

Figure SPM.1 | Total annual anthropogenic GHG emissions ($GtCO_2eq/yr$) by groups of gases 1970–2010: CO_2 from fossil fuel combustion and industrial processes; CO_2 from Forestry and Other Land Use (FOLU); methane (CH_4); nitrous oxide (N_2O); fluorinated gases[8] covered under the Kyoto Protocol (F-gases). At the right side of the figure GHG emissions in 2010 are shown again broken down into these components with the associated uncertainties (90 % confidence interval) indicated by the error bars. Total anthropogenic GHG emissions uncertainties are derived from the individual gas estimates as described in Chapter 5 [5.2.3.6]. Global CO_2 emissions from fossil fuel combustion are known within 8 % uncertainty (90 % confidence interval). CO_2 emissions from FOLU have very large uncertainties attached in the order of ±50 %. Uncertainty for global emissions of CH_4, N_2O and the F-gases has been estimated as 20 %, 60 % and 20 %, respectively. 2010 was the most recent year for which emission statistics on all gases as well as assessment of uncertainties were essentially complete at the time of data cut-off for this report. Emissions are converted into CO_2-equivalents based on GWP_{100}[6] from the IPCC Second Assessment Report. The emission data from FOLU represents land-based CO_2 emissions from forest fires, peat fires and peat decay that approximate to net CO_2 flux from FOLU as described in Chapter 11 of this report. Average annual growth rate over different periods is highlighted with the brackets. [Figure 1.3, Figure TS.1]

Greenhouse Gas Emissions by Economic Sectors

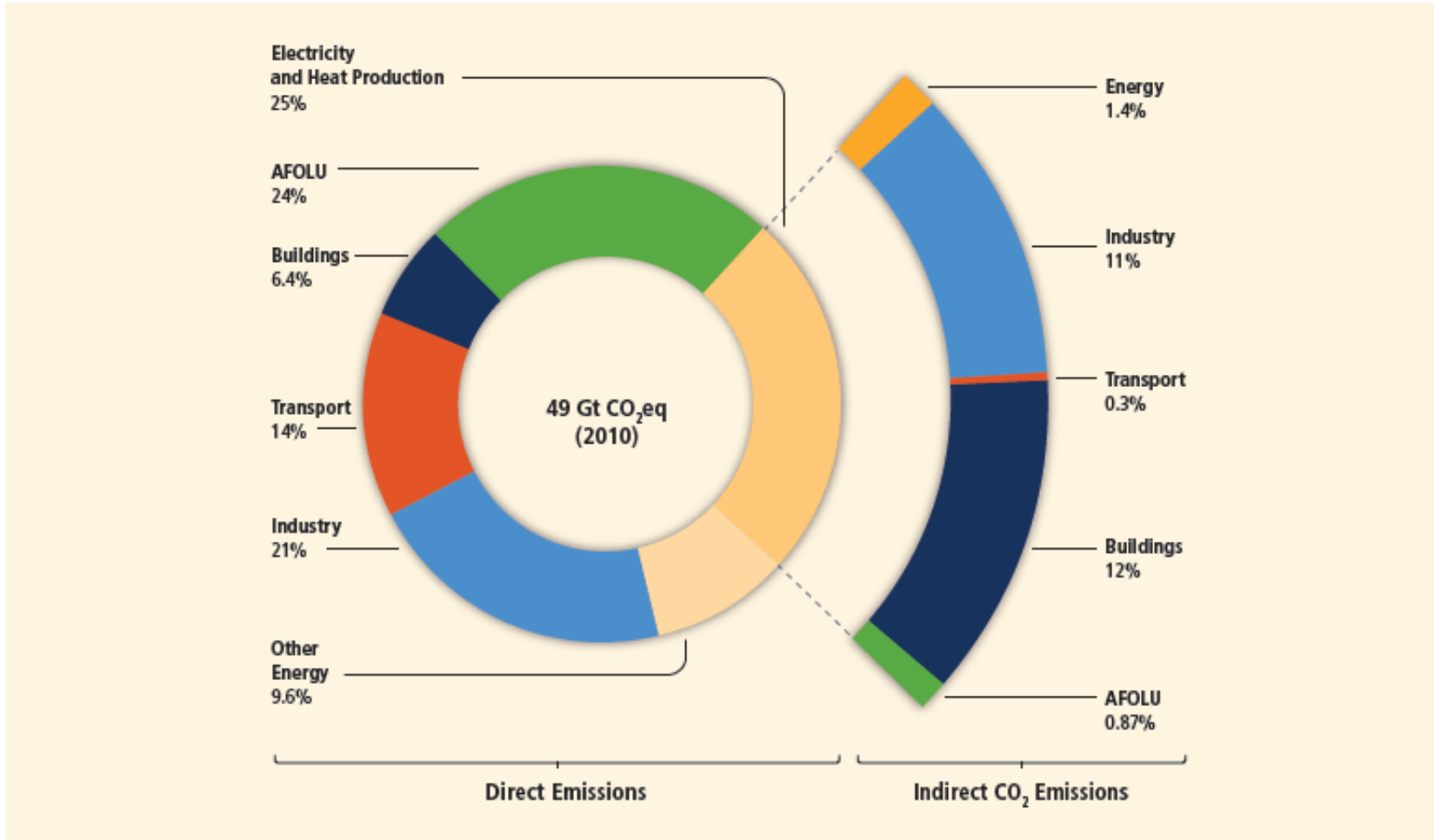

Figure SPM.2| Total anthropogenic GHG emissions ($GtCO_2eq/yr$) by economic sectors. Inner circle shows direct GHG emission shares (in % of total anthropogenic GHG emissions) of five economic sectors in 2010. Pull-out shows how indirect CO_2 emission shares (in % of total anthropogenic GHG emissions) from electricity and heat production are attributed to sectors of final energy use. 'Other Energy' refers to all GHG emission sources in the energy sector as defined in Annex II other than electricity and heat production [A.II.9.1]. The emissions data from Agriculture, Forestry and Other Land Use (AFOLU) includes land-based CO_2 emissions from forest fires, peat fires and peat decay that approximate to net CO_2 flux from the Forestry and Other Land Use (FOLU) sub-sector as described in Chapter 11 of this report. Emissions are converted into CO_2-equivalents based on GWP_{100}[6] from the IPCC Second Assessment Report. Sector definitions are provided in Annex II.9. [Figure 1.3a, Figure TS.3 upper panel]

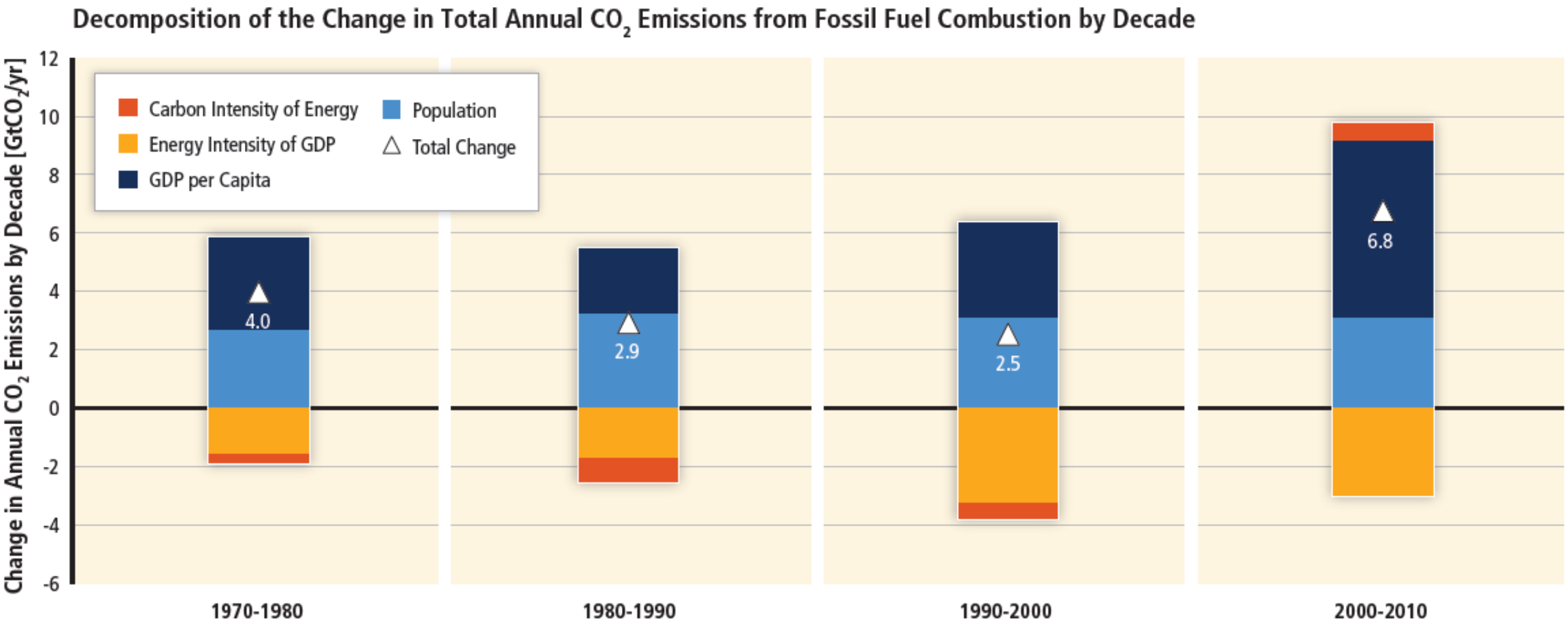

Figure SPM.3| Decomposition of the change in total annual CO_2 emissions from fossil fuel combustion by decade and four driving factors: population, income (GDP) per capita, energy intensity of GDP and carbon intensity of energy. The bar segments show the changes associated with each factor alone, holding the respective other factors constant. Total emissions changes are indicated by a triangle. The change in emissions over each decade is measured in gigatonnes of CO_2 per year [$GtCO_2$/yr]; income is converted into common units using purchasing power parities. [Figure 1.7]

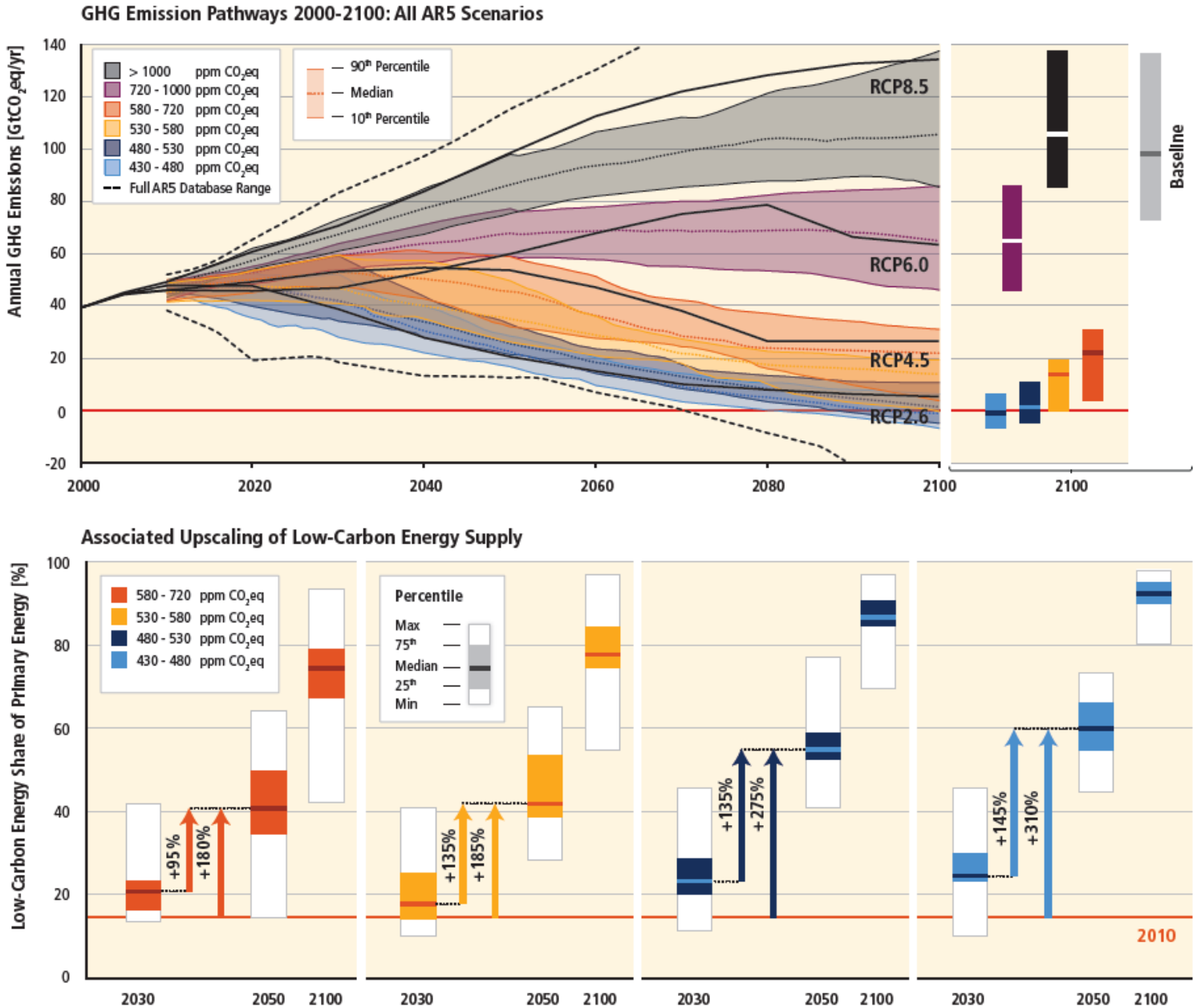

Figure SPM.4 | Pathways of global GHG emissions ($GtCO_2eq/yr$) in baseline and mitigation scenarios for different long-term concentration levels (upper panel) [Figure 6.7] and associated upscaling requirements of low-carbon energy (% of primary energy) for 2030, 2050 and 2100 compared to 2010 levels in mitigation scenarios (lower panel) [Figure 7.16]. The lower panel excludes scenarios with limited technology availability and exogenous carbon price trajectories. For definitions of CO_2-equivalent emissions and CO_2-equivalent concentrations see the WGIII AR5 Glossary.